

Studying the geometry of the emitting region in X-ray binaries using optical and X-ray polarimetry or How to see the Unseen

Juri Poutanen

(University of Turku, Finland)

October 10, 2024

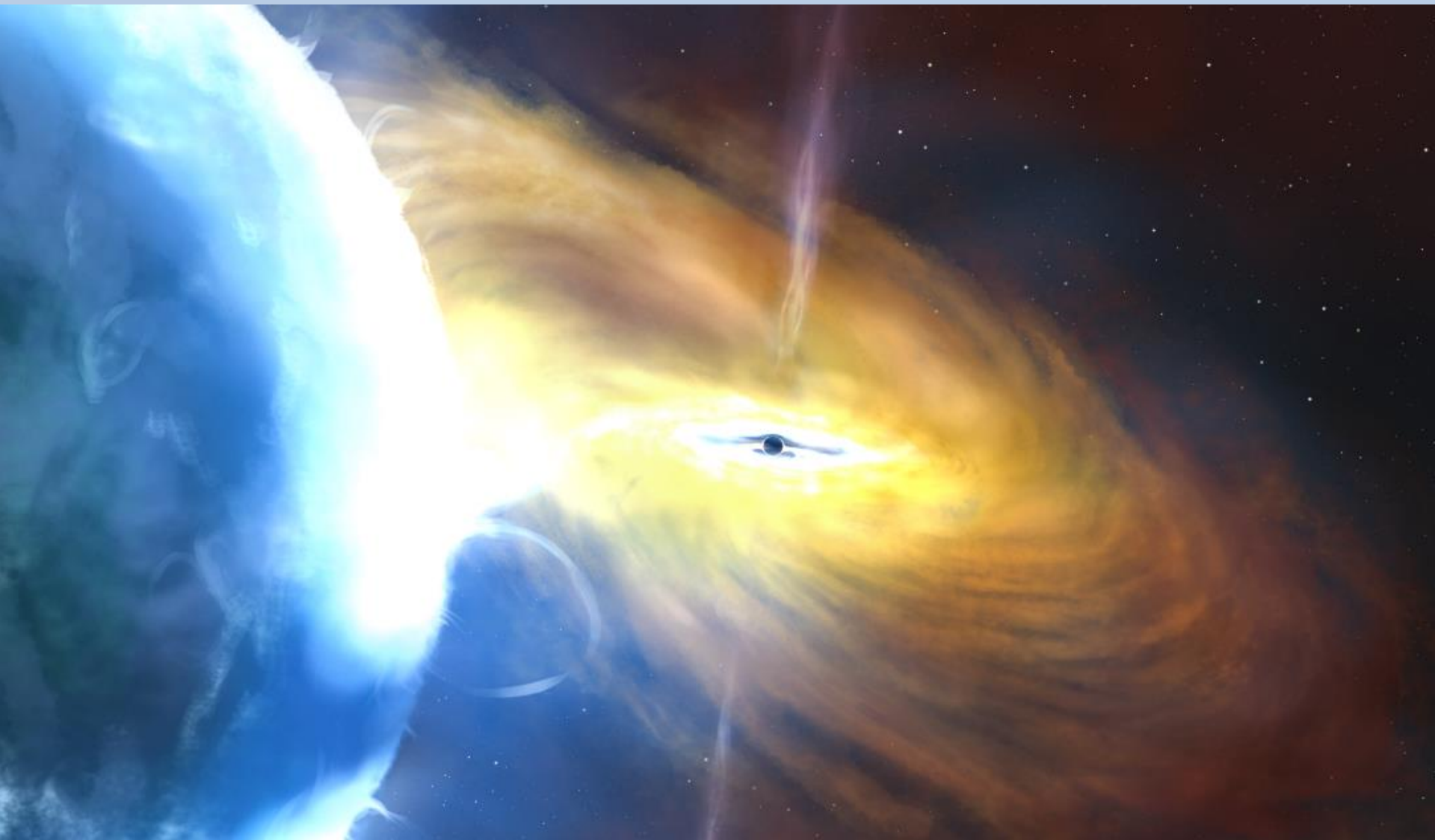
References to reviews:

1. Poutanen et al. 2024, *Galaxies*, 12, 46
2. Ursini et al. 2024, *Galaxies*, 12, 43
3. Dovciak et al. 2024, *Galaxies*, in press

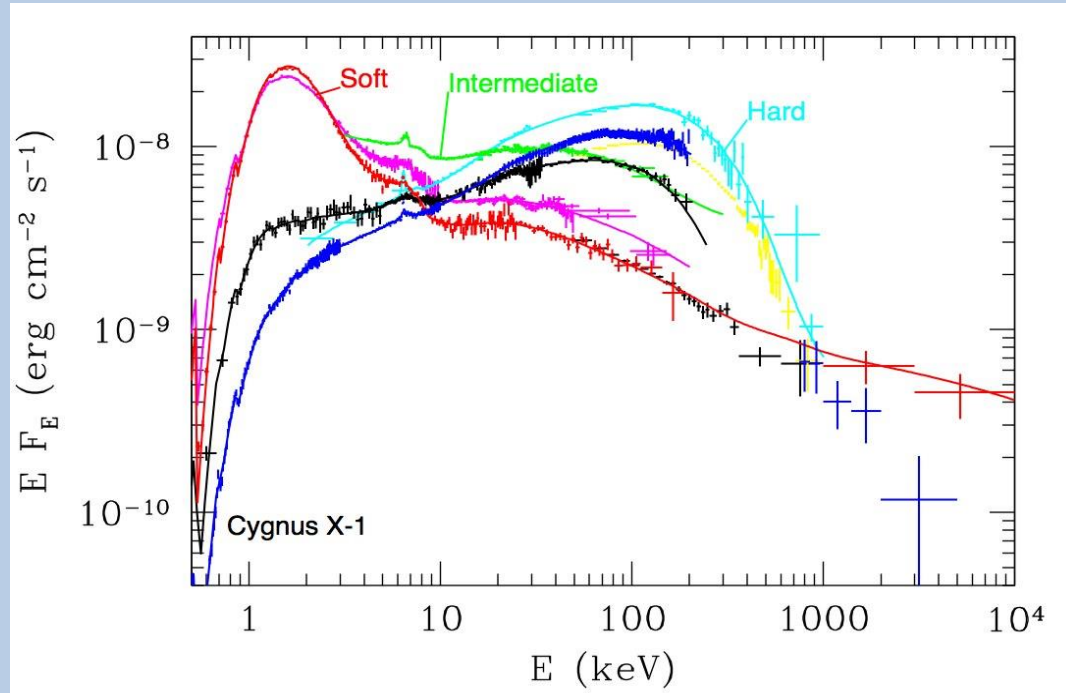


IXPE
Imaging
X-Ray
Polarimetry
Explorer

Stellar-mass black holes



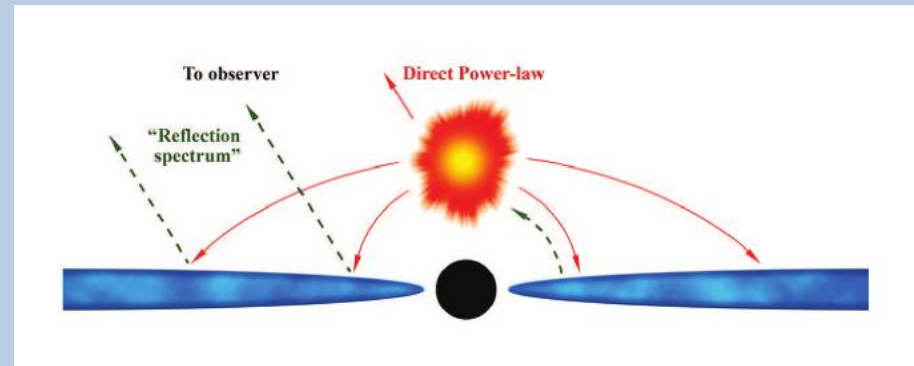
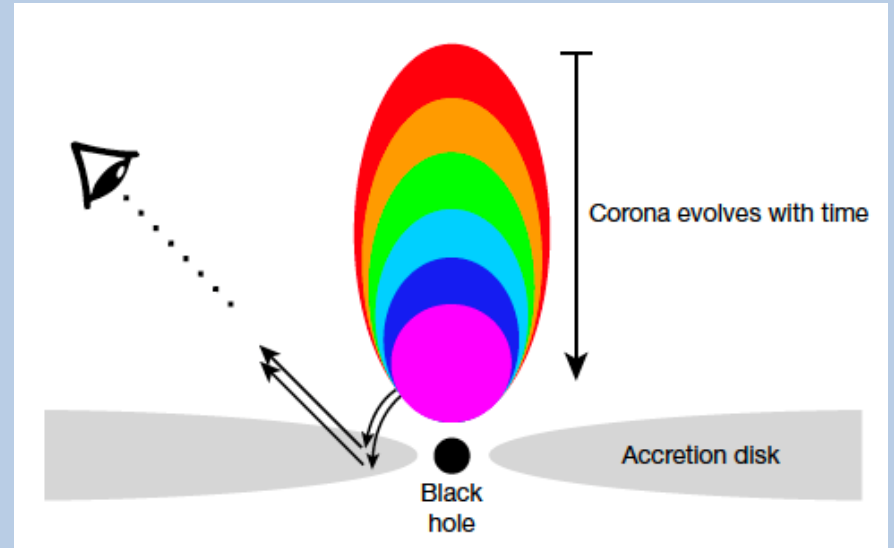
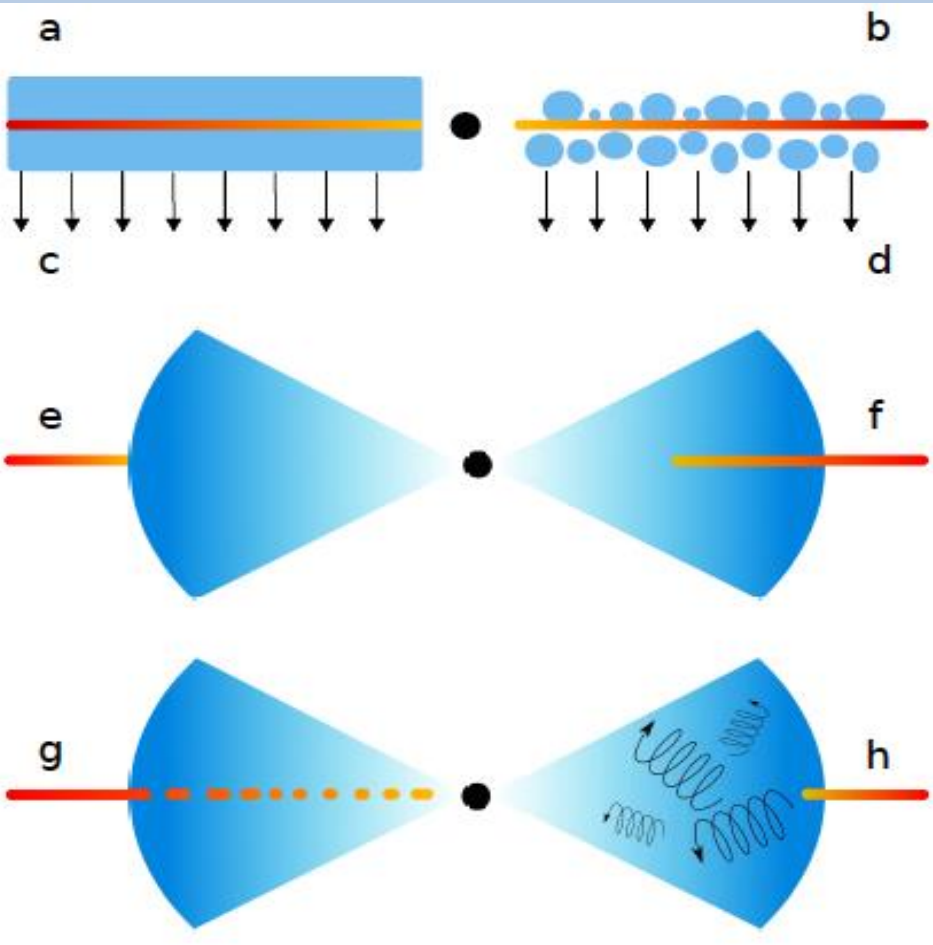
Cygnus X-1 hard state geometry



The hard state spectrum is produced by multiply Compton scattering (thermal Comptonization). However, the geometry of emission region is unknown.

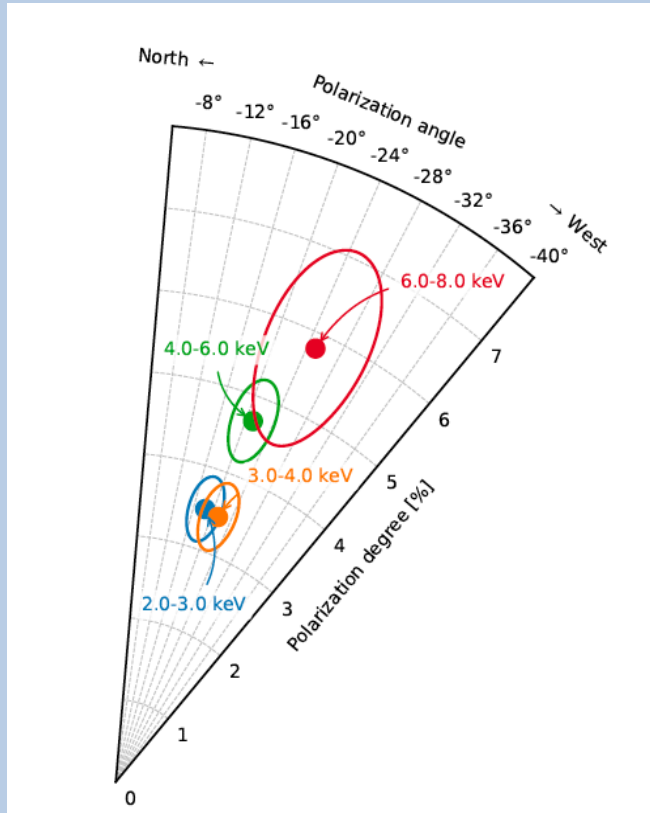
Polarization is sensitive to the geometry of the "corona", its dynamics and source of seed photons

Cygnus X-1 hard state geometry

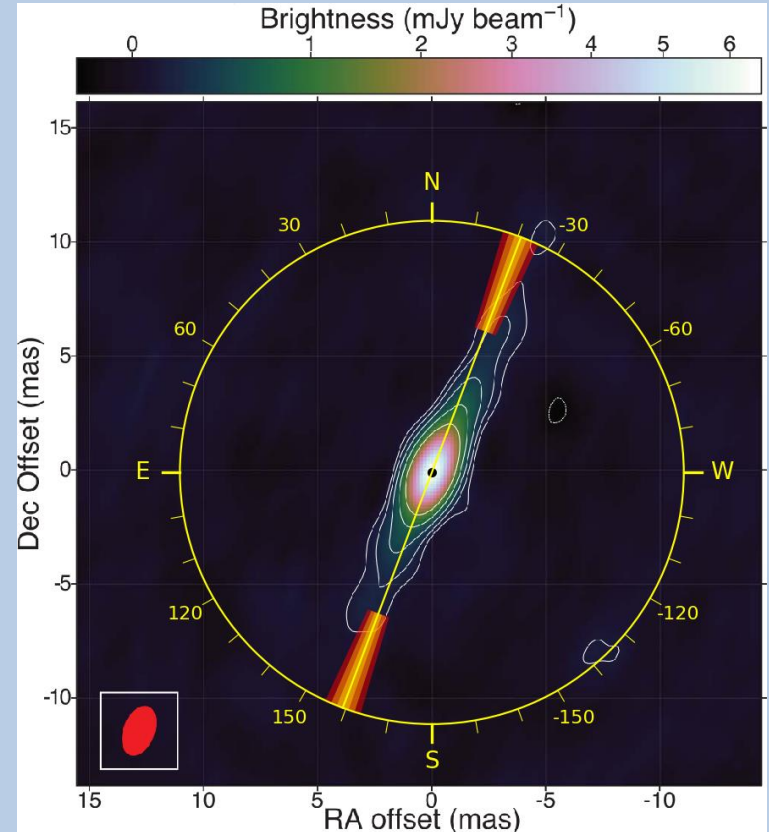


Cygnus X-1

- IXPE observed Cyg X-1 in the hard state in May and June 2022.

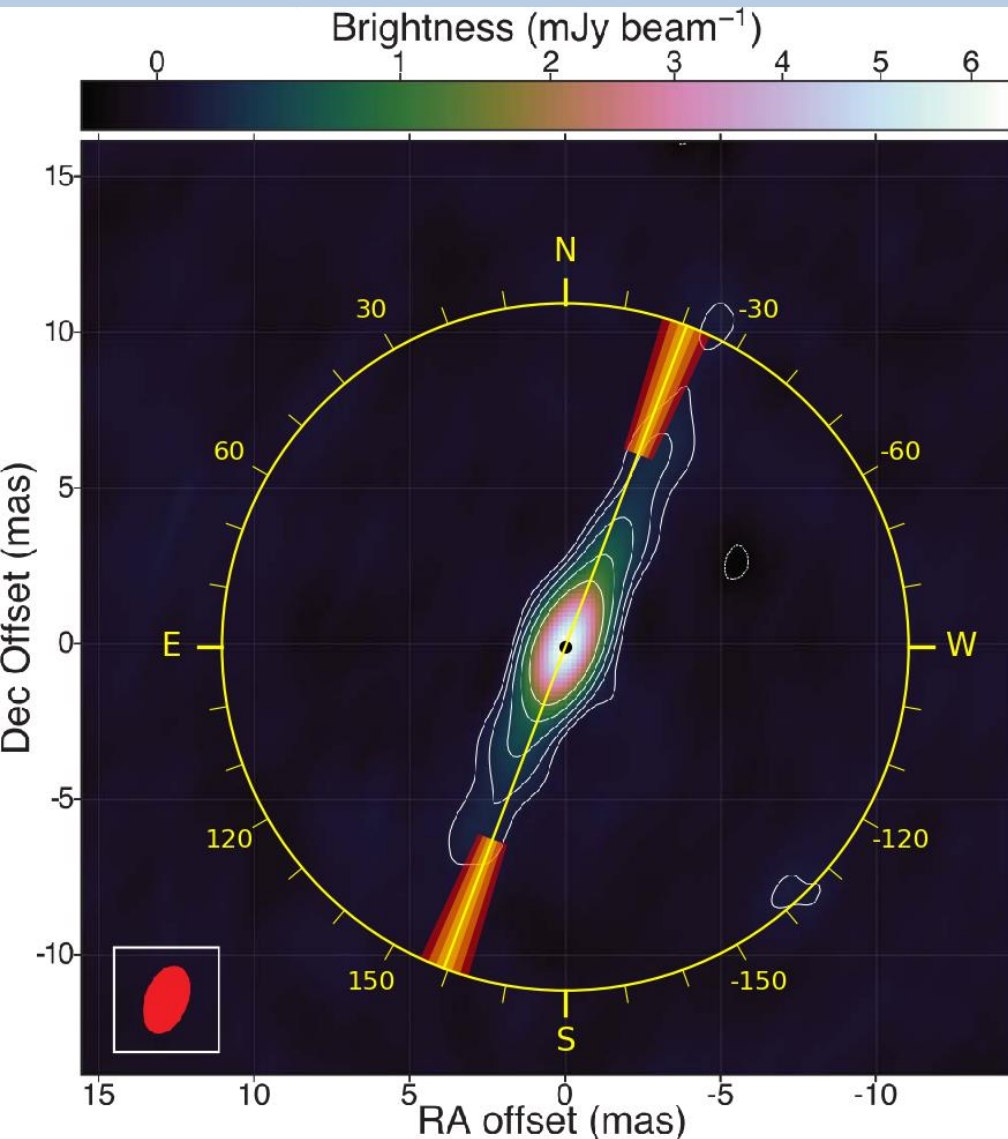


$PD = 4.0 \pm 0.2 \%$
 $PA = -20.7 \pm 1.4 \text{ deg}$

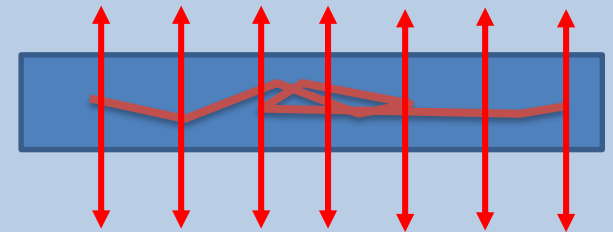


X-ray polarization
 parallel to the jet

Cygnus X-1



X-ray polarization parallel to the jet
 \Rightarrow X-ray emitting region is elongated
 perpendicular to the jet.

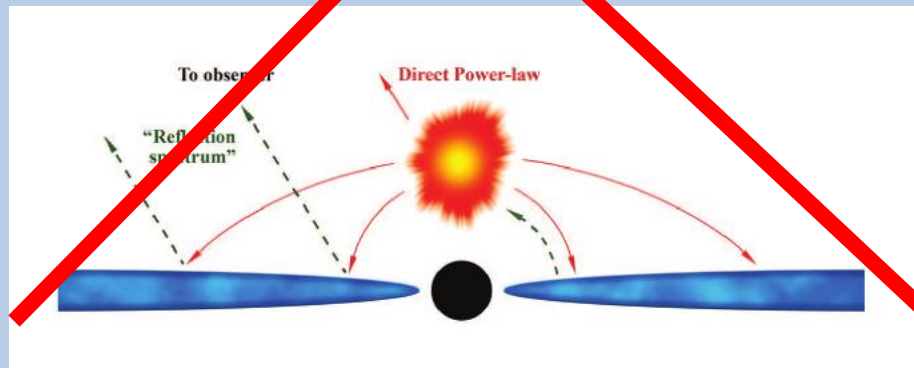
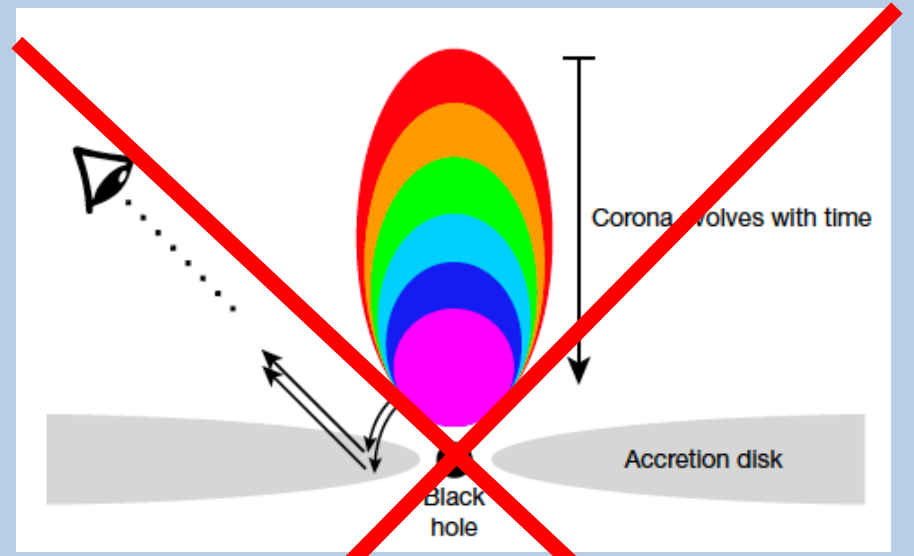
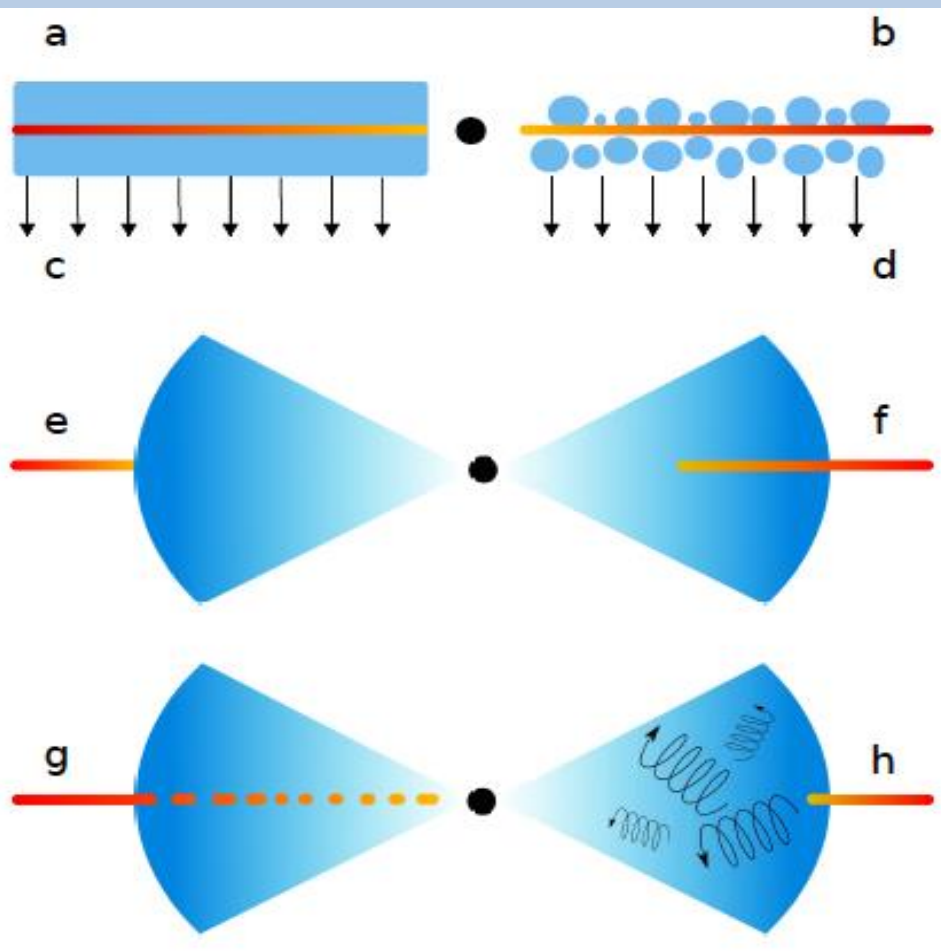


Polarization is perpendicular to the
 disk. Scattering in the optically thin
 slab produces polarization normal
 to the scattering plane.

- Optical (intrinsic) polarization
 has the same angle \Rightarrow orbit
 perpendicular to the jet.
- How to get 4% polarization?

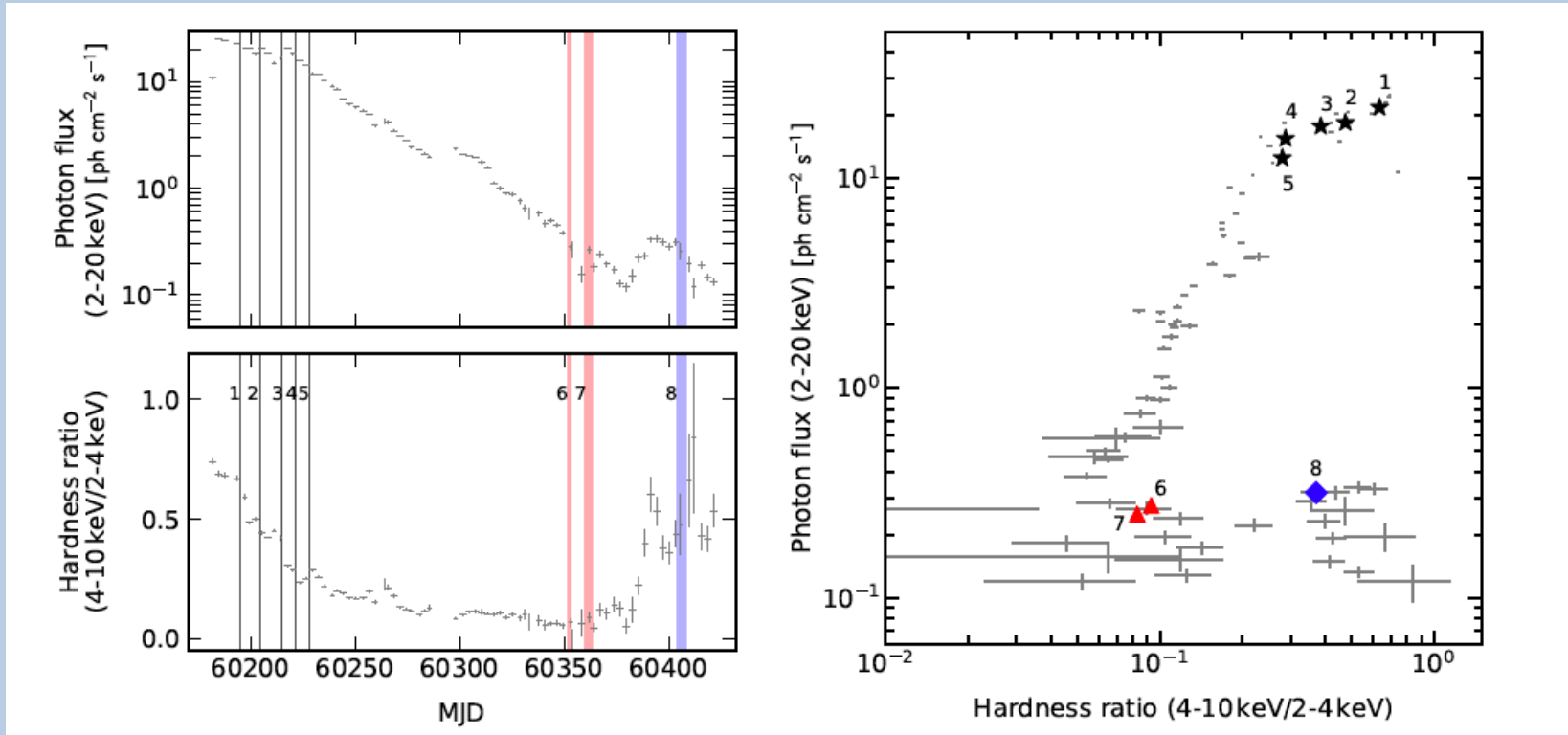
Hard state geometry

Jet and lamp-post models are rejected

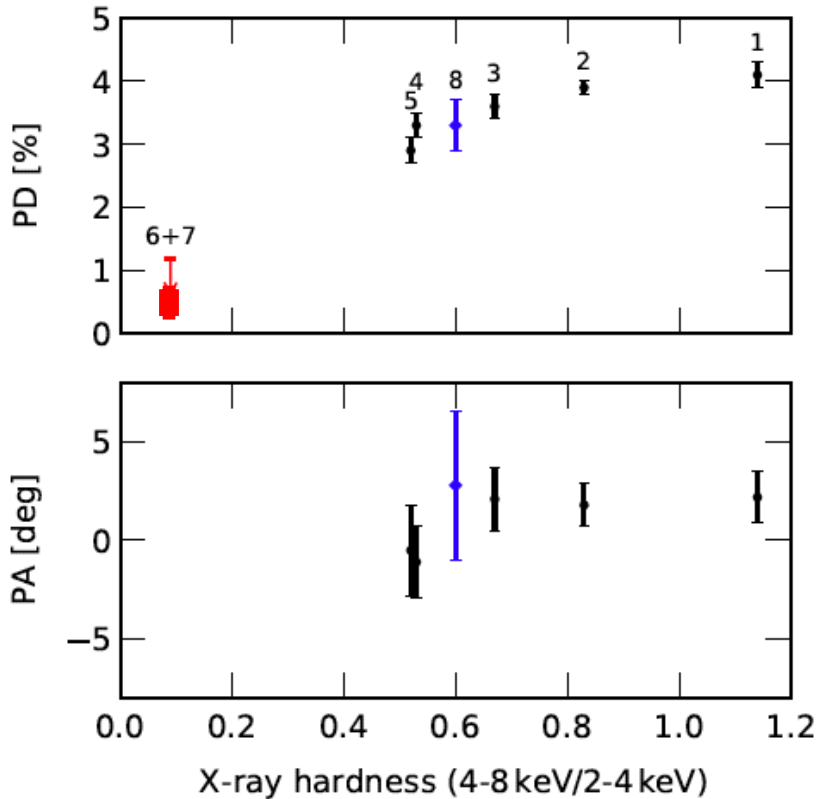


Swift J1727.8–1613

Outburst starting from August 2023



Swift J1727.8–1613



In the hard state

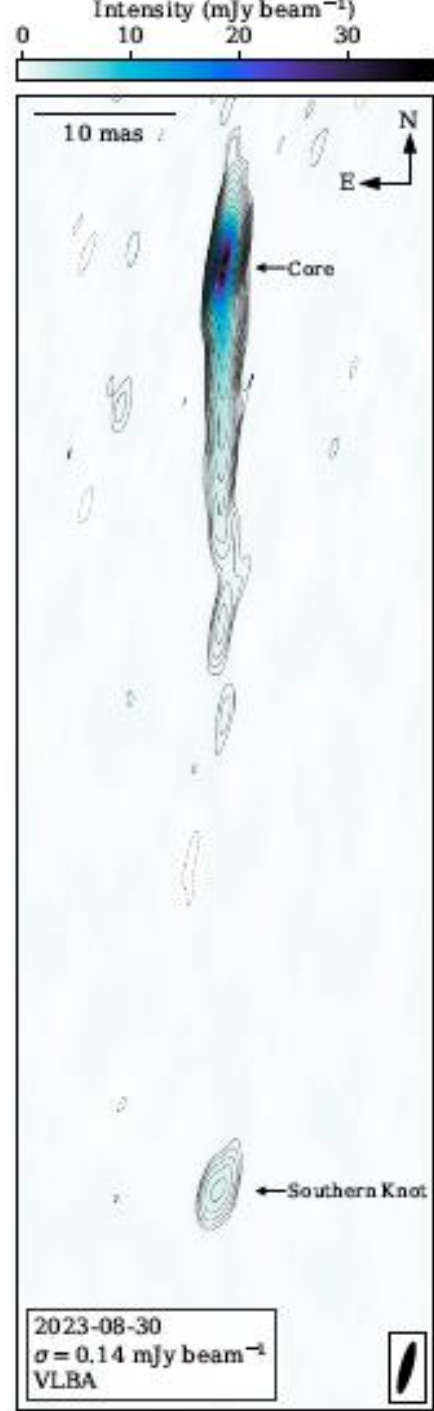
PD=4.1±0.2%, PA=2.2±1.3 deg

Sub-mm PA= -4.1±3.5 deg

We predicted jet to be directed along position angle 0.

And was measured at -0.60 ± 0.07 deg (Wood+2024)

Swift J172

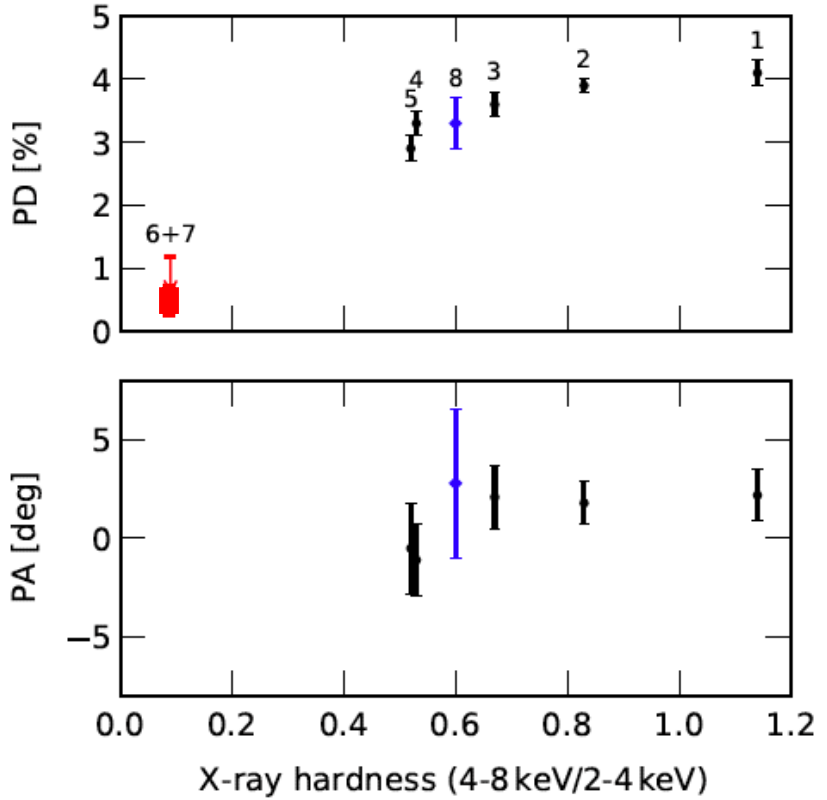


In the
 PD=4.
 Sub-m
 We pr
 positio

And w
 (Wood

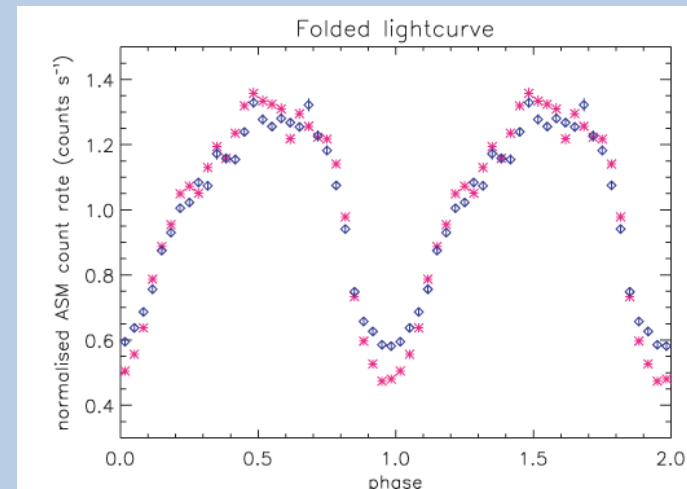
along

07 deg



Cygnus X-3

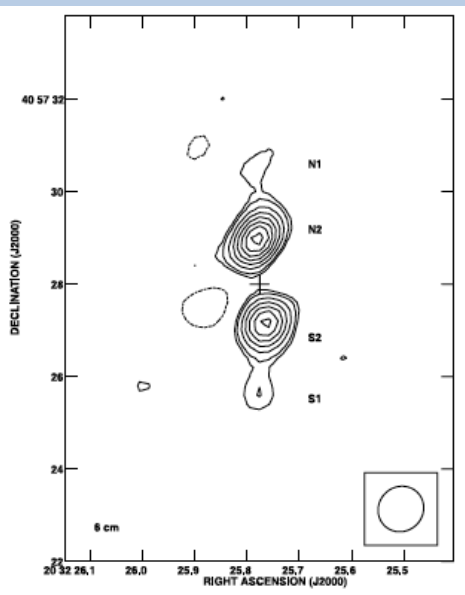
- Discovered in X-rays in 1966 (Giacconi et al. 1967)
- High ISM absorption, no optical counterpart; IR orbital variability and polarization.
- Distance 7.4 ± 1.1 kpc
- X-ray orbital modulations with orbital period $P_{\text{orb}} = 4.8^{\text{h}}$.
- Also IR modulation and IR and X-ray lines all indicate the same orbital period. Inclination $i = 29.5^\circ \pm 1.2^\circ$ from IR and X-ray photometric orbital variability from absorption (Antokhin et al. 2022).
- The only Galactic source with a compact object in a binary orbit with a Wolf-Rayet companion; progenitor of the double degenerate system, similar to LIGO targets (Belczynski et al. 2013)



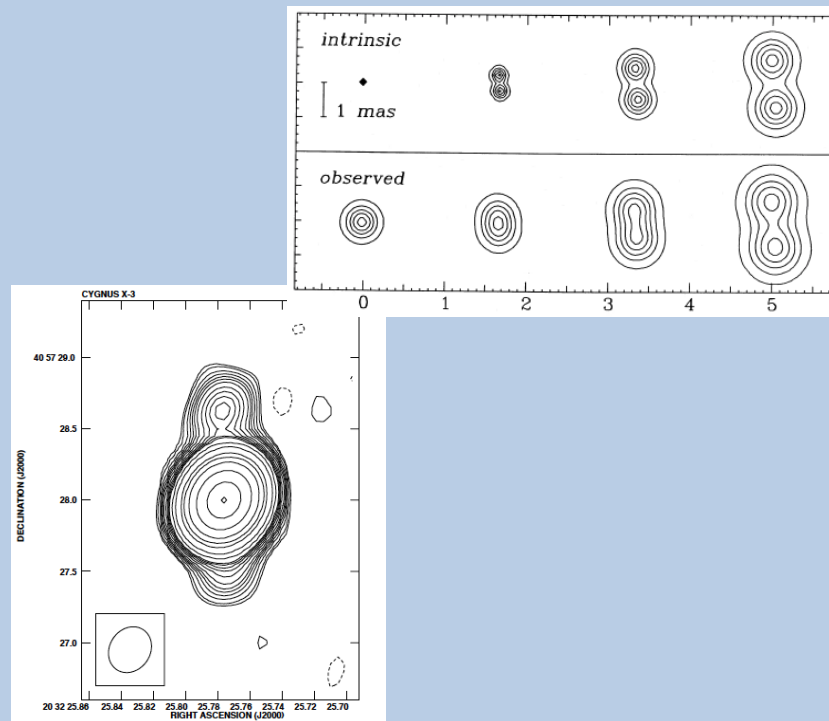
Cygnus X-3

- Radio counterpart (Braes & Miley 1972), among the brightest radio sources (detected fluxes as high as 20 Jy, Corbel et al. 2013)
- N-S orientation of radio ejections

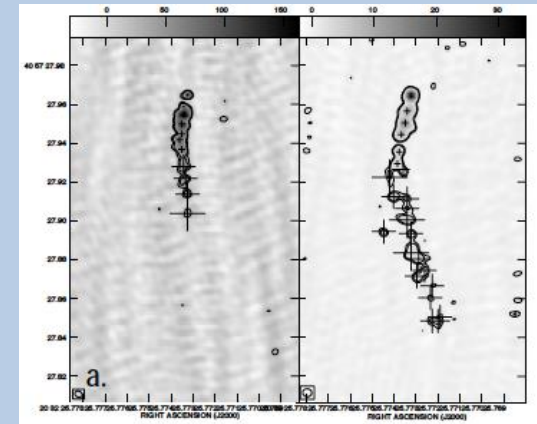
Marti et al. 2001



Molnar et al. 1988

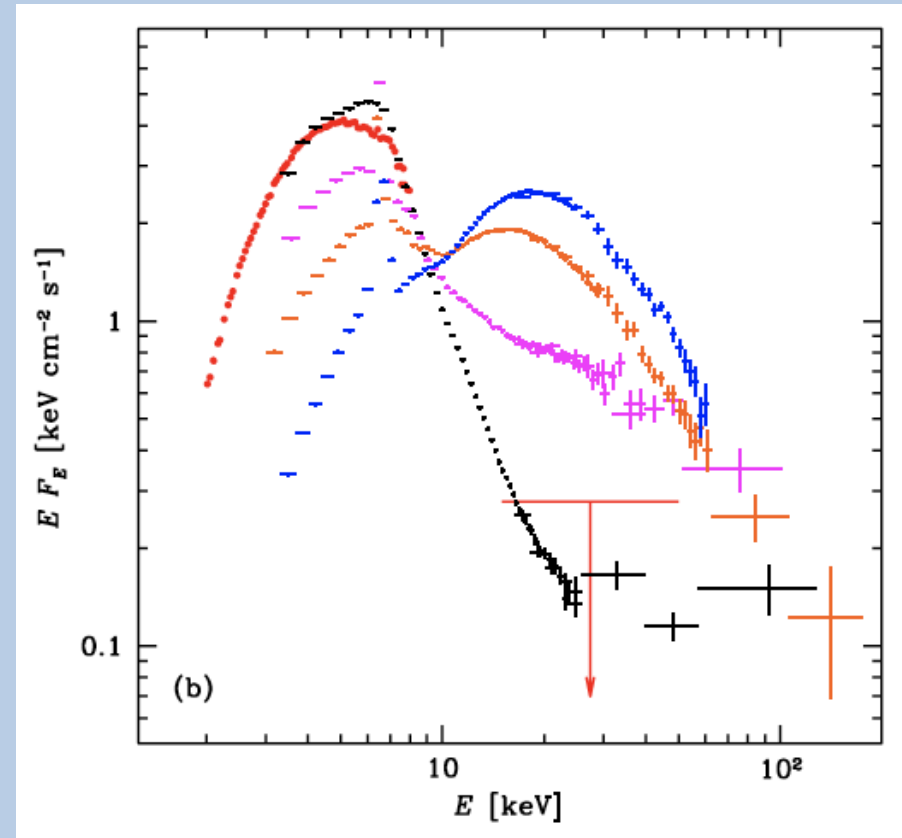
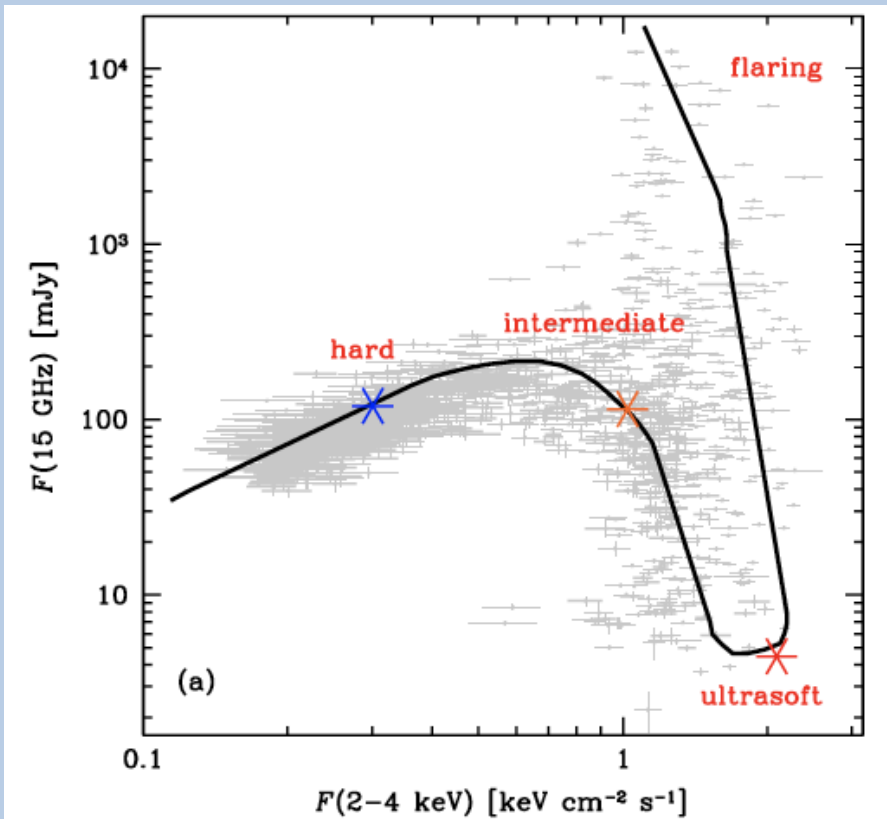


Mioduszewski et al. 2001



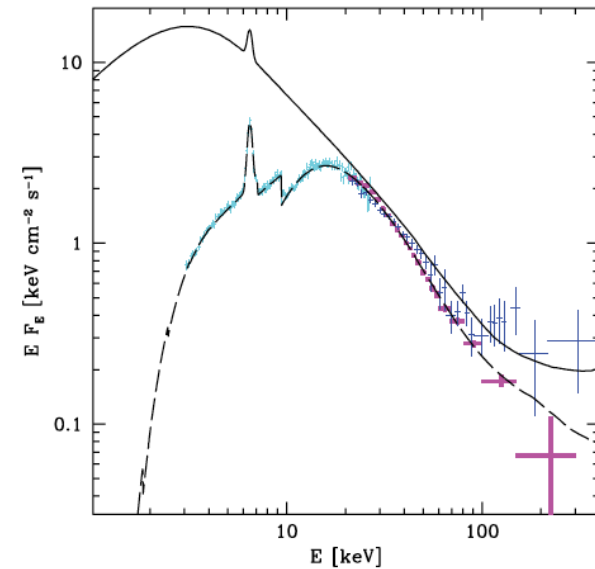
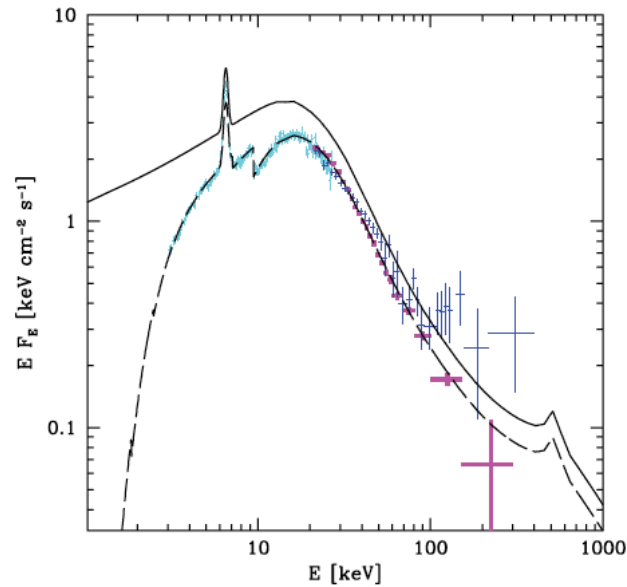
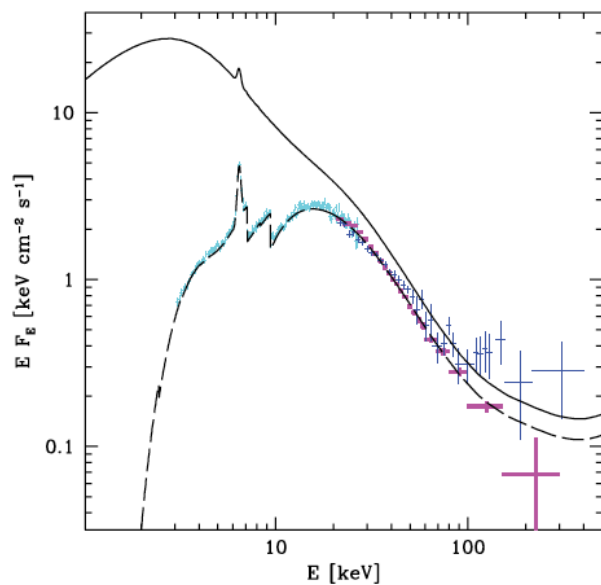
Cygnus X-3

- Spectral transitions from hard (with strong iron line) to very soft, blackbody-like.
- Often compared to the other accreting high-mass BH X-ray binary Cyg X-1, but is not quite the same.

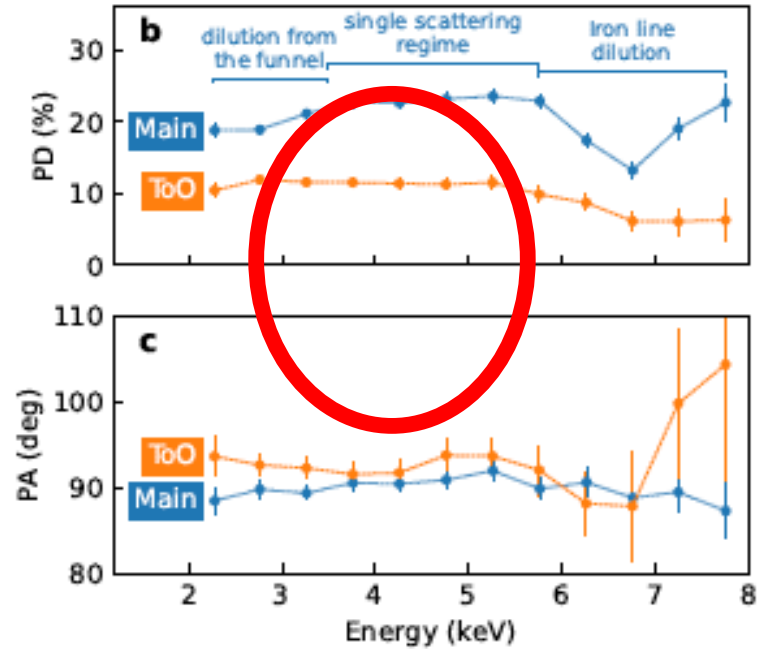
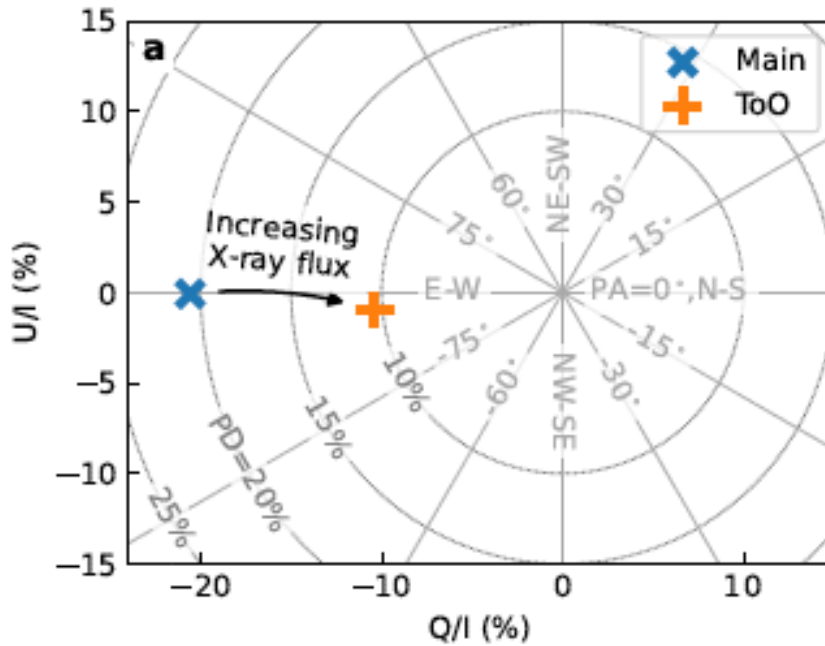


Cygnus X-3

- Spectral modelling is uncertain, e.g., the hard-state spectra can be explained with (i) soft spectrum, severely absorbed by WR wind; (ii) standard hard spectrum; (iii) reflection-dominated spectrum (Hjalmarsdotter et al. 2009, Zdziarski et al. 2010).



IXPE observations of Cygnus X-3



Main observation: 14-19 Oct, 31 Oct-6 Nov 2022

ToO observation: 25-29 Dec 2022

PD = 20.6 +/- 0.3 %

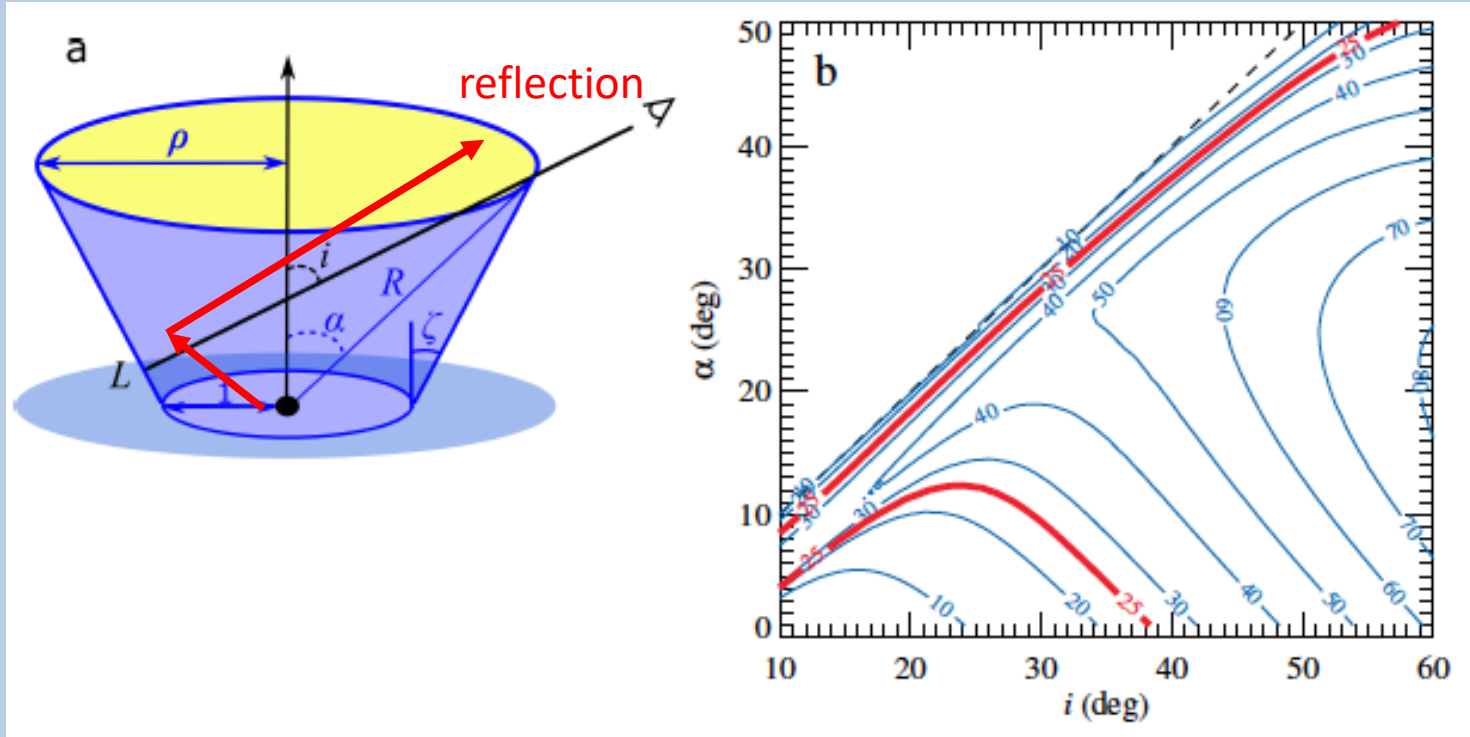
PA = 90.1 +/- 0.4°

PA perpendicular to the jet!

PD = 10.4 +/- 0.3 %

PA = 92.6 +/- 0.7°

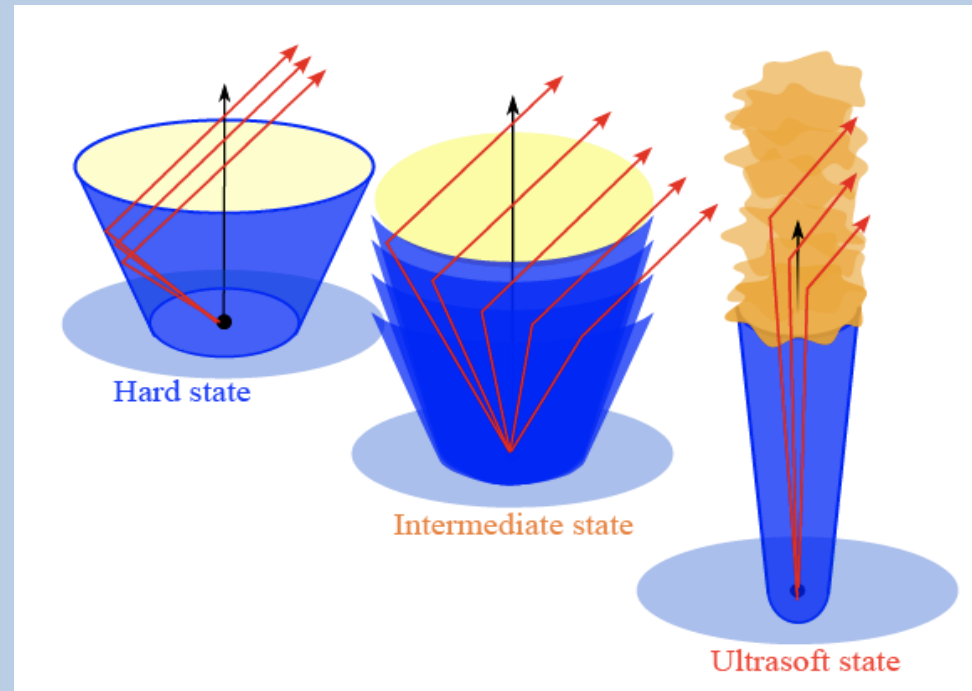
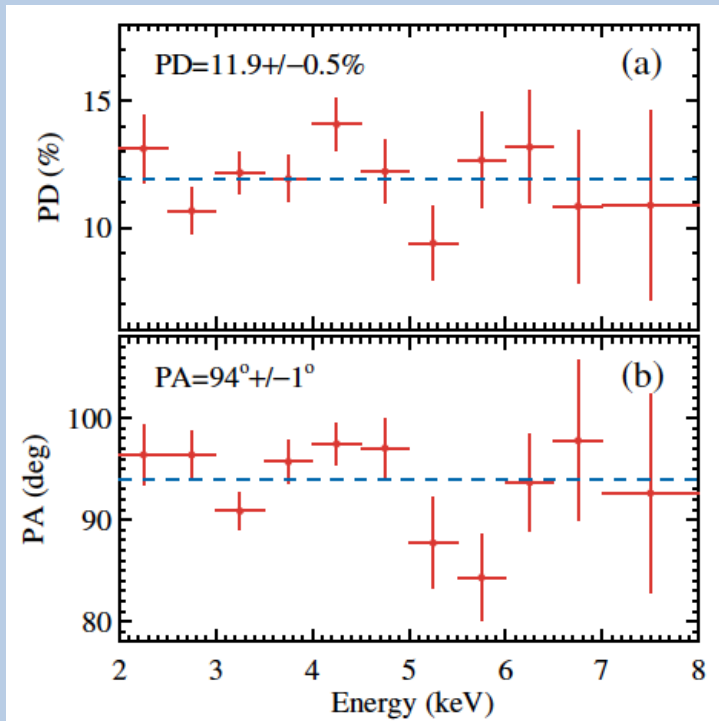
X-ray polarization: reflection from a funnel



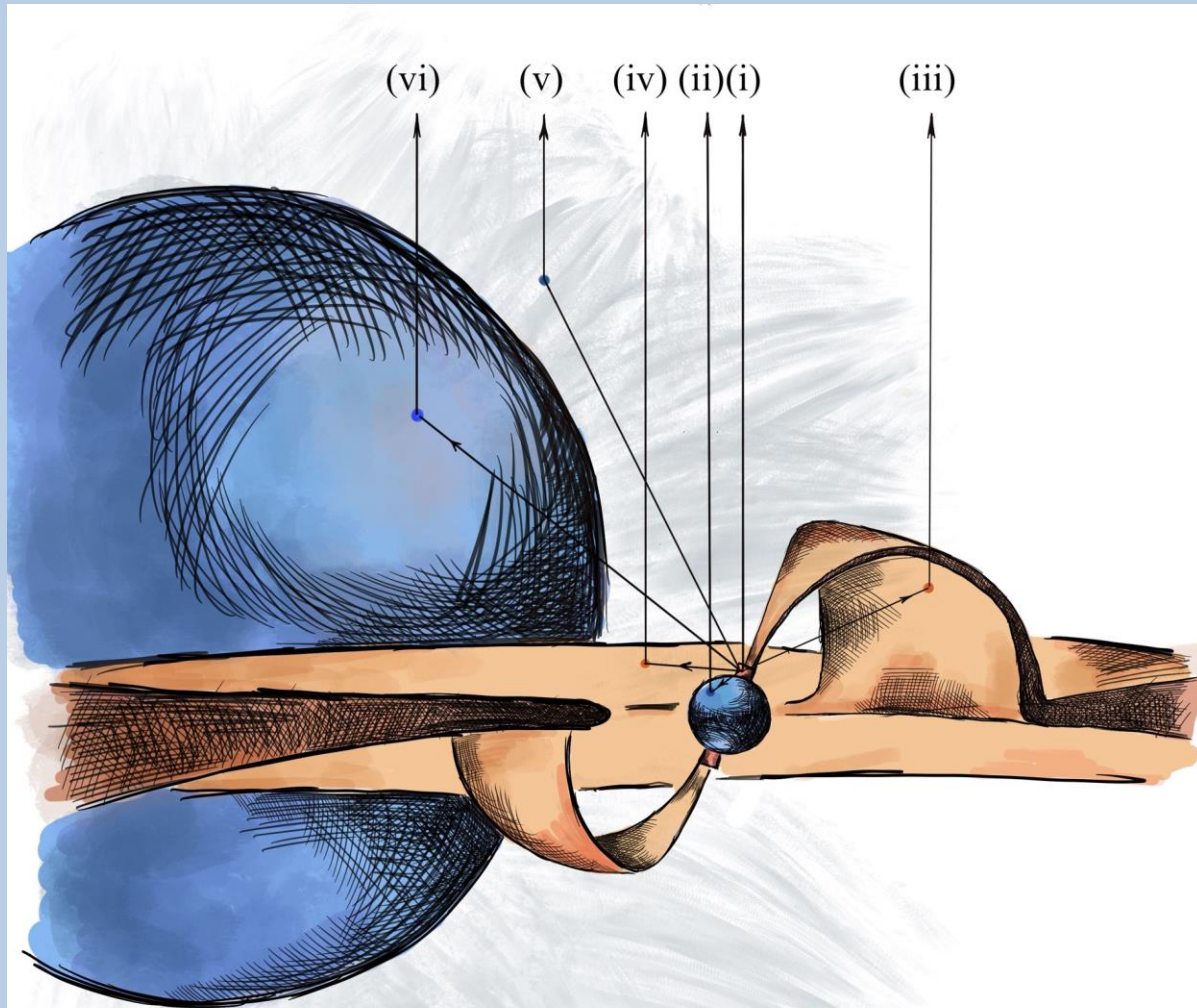
- PA \perp jet (/binary axis). High PD: we do not see central source
- $i \approx 30^\circ$ hence optically thick matter high above the disc.
- Modelling gives high intrinsic luminosity in excess 10^{39} erg/s.
- **Cygnus X-3 is a hidden ULX !**

X-ray polarization: reflection from a funnel

- In the (ultra-)soft state, the spectrum is blackbody-like, very weak iron line, the PD was expected to be very low.
- However, it turned out to be $PD=12\%$ at nearly the same $PA=94^\circ$. No energy dependence (in particular around Fe line).



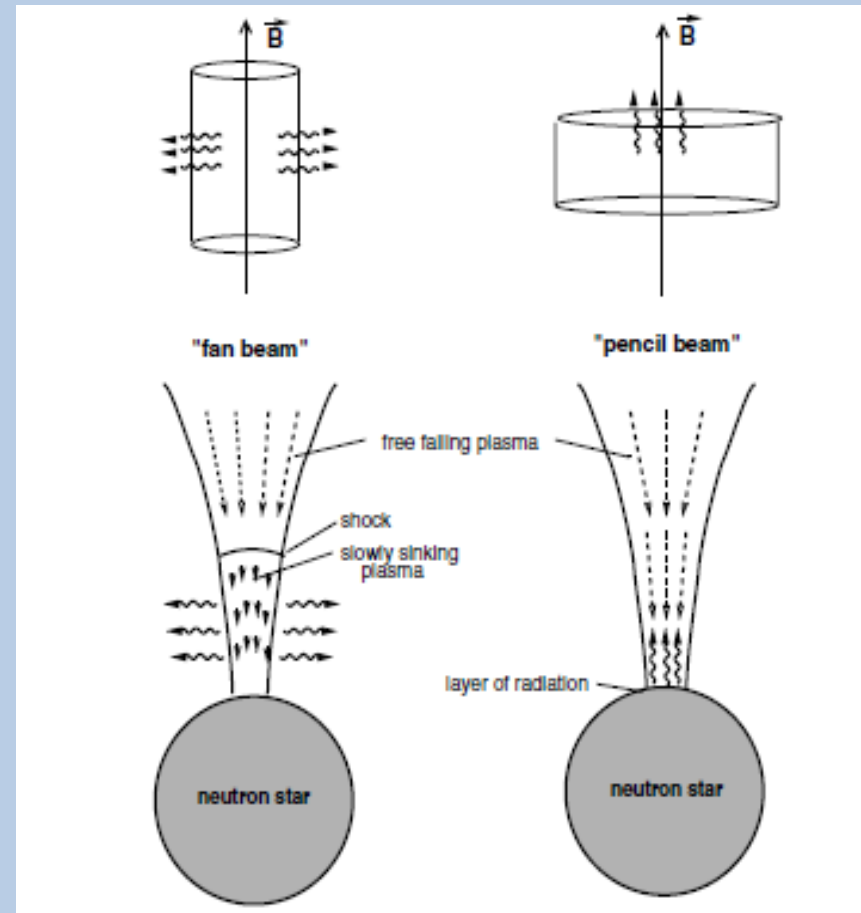
X-ray pulsars



X-ray pulsars

Main goals

- Determining geometry of the emitting region (hotspot vs column) and emission pattern (fan vs pencil beam) at different luminosity levels
- Revealing evidence for non-dipolar fields
- Test free-precession model for Her X-1



Meszáros et al. 1988

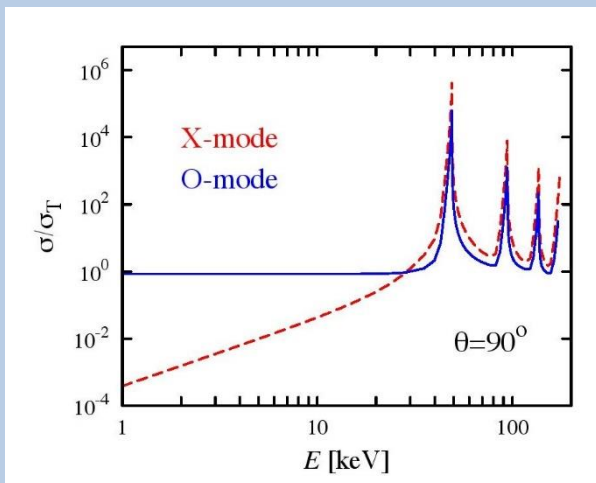
X-ray pulsars

Opacity in highly magnetized plasma:

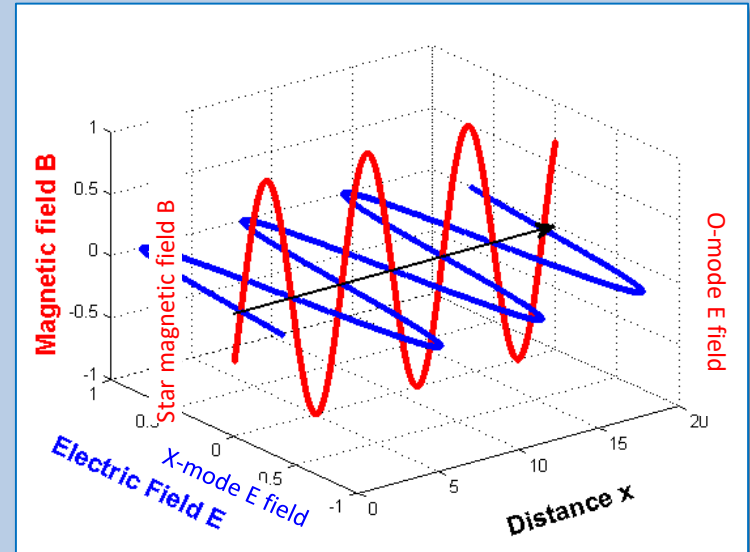
$$k_{\perp} \approx (E/E_B)^2 k_{\parallel} \quad E < E_B = 11.6 (B_{12}) \text{ keV}$$

(electron cyclotron energy)

where k_{\perp} and (k_{\parallel}) are the opacities in the Extraordinary (Ordinary) modes, when the wave electron field is perpendicular (parallel) to the plane defined by the line of propagation and the external magnetic field



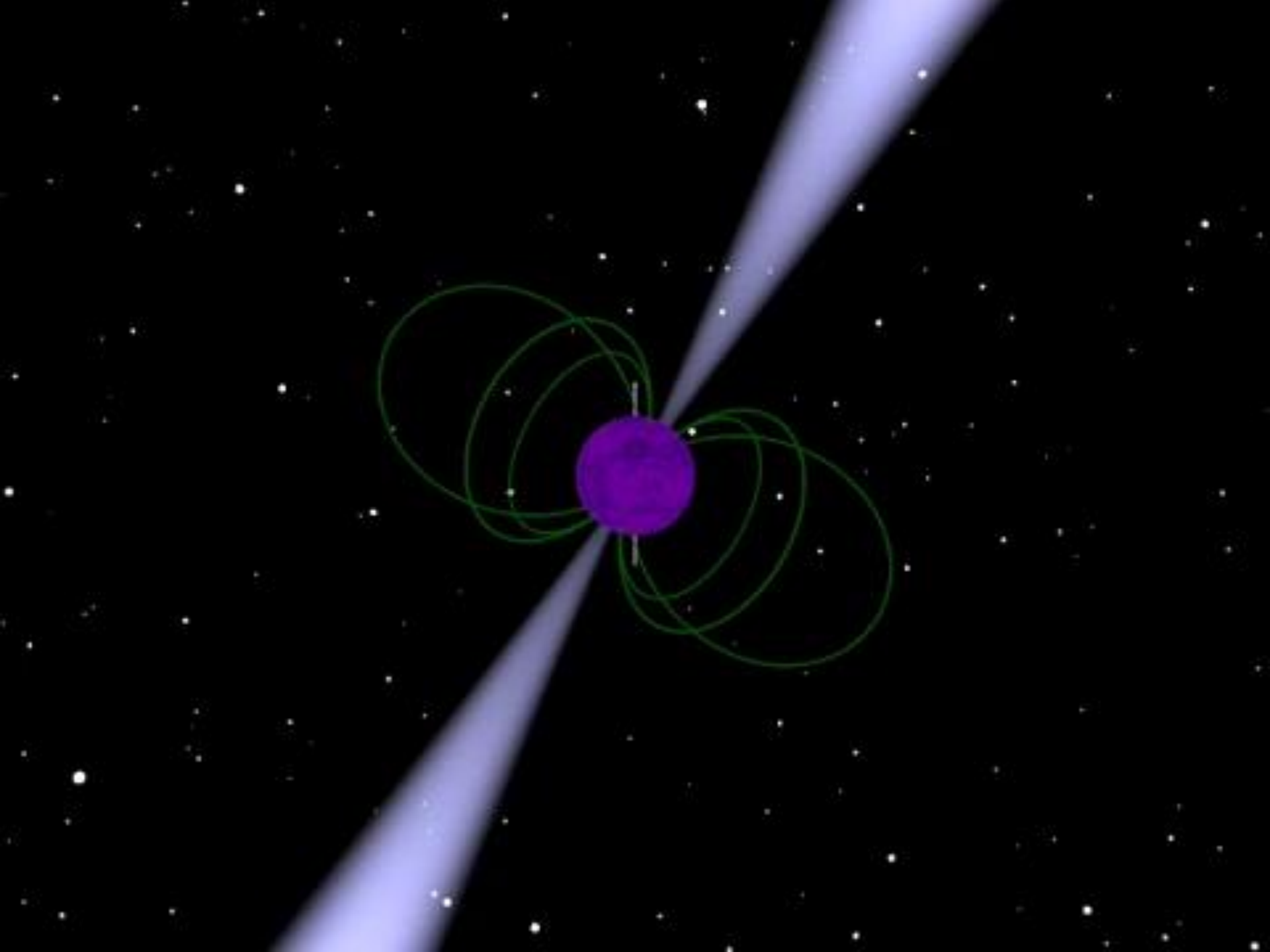
Mushtukov et al. 2016



O-mode: the E-field oscillates in the **k-B** plane
X-mode: the E-field oscillates \perp to the **k-B** plane

IXPE: X-ray pulsars

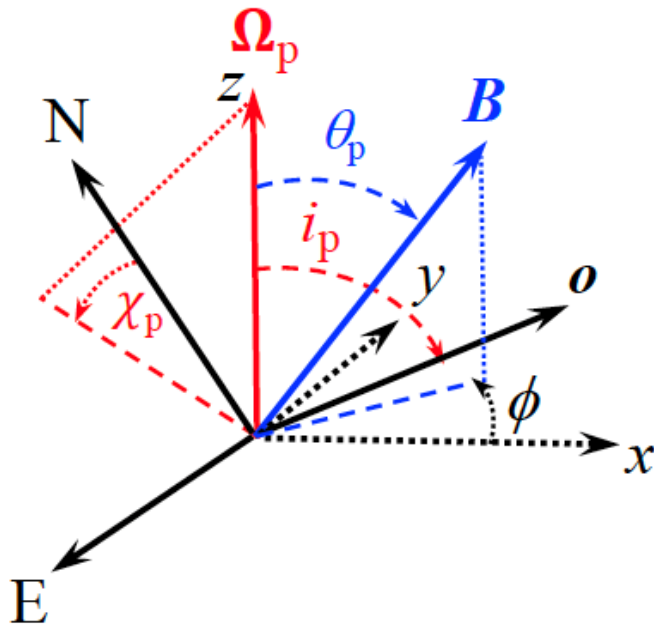
Name	Spin Period ^{a,b} [s]	Orbital Period ^{a,b} [d]	Distance ^{a,b} [kpc]	Luminosity ^c [erg s ⁻¹]	CRSF ^d [keV]
Cen X-3	4.8	2.09	6.07	1.9×10^{37}	28
Her X-1	1.24	1.7	7.09	$\sim 3 \times 10^{37}$	37
4U 1626-67	7.7	0.02875	15.08	6.4×10^{36}	37, 61?
Vela X-1	283	8.96	1.87	3.8×10^{35}	25, 53
GRO J1008-57	93.5	249.5	3.21	$(0.6 - 1.6) \times 10^{36}$	78
EXO 2030+375	41.31	46.02	2.08	1.3×10^{36}	36/63?
X Persei	837.67	250.3	0.63	1.2×10^{34}	29
GX 301-2	696.0	41.59	3.54	1.3×10^{36}	37/50
LS V +44 17	202.5	155.0	2.29	$\leq 4 \times 10^{37}$	32
Swift J0243.6+6124	9.87	28.3	5.2	$(0.6 - 2.4) \times 10^{37}$	146
SMC X-1	0.717	3.892	61	2×10^{38}	-



Rotating Vector Model (RVM)

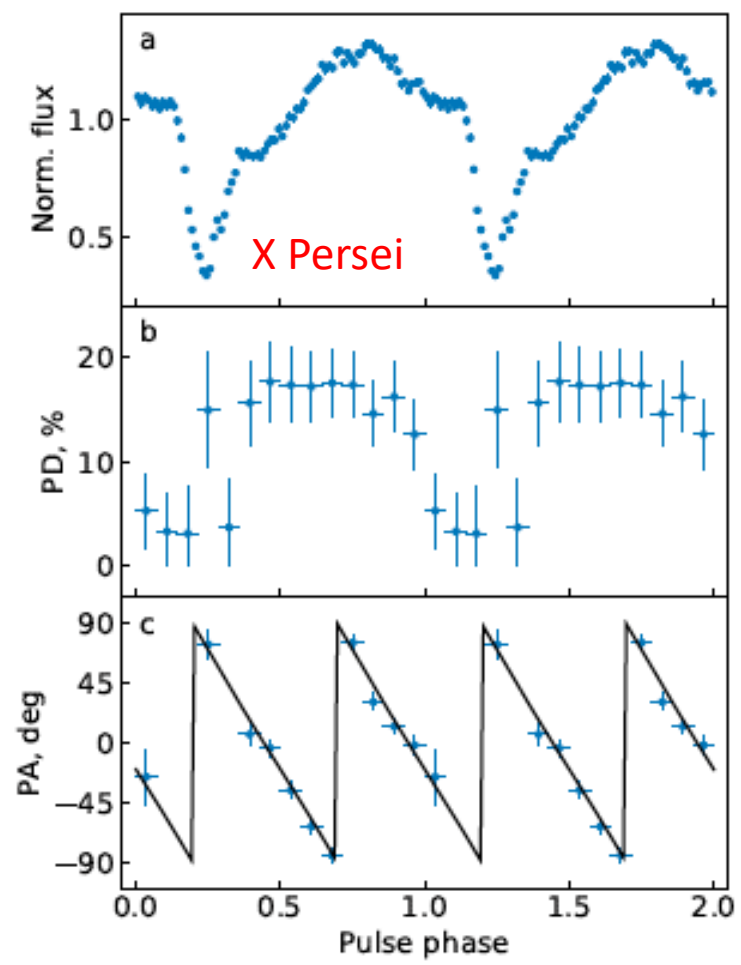
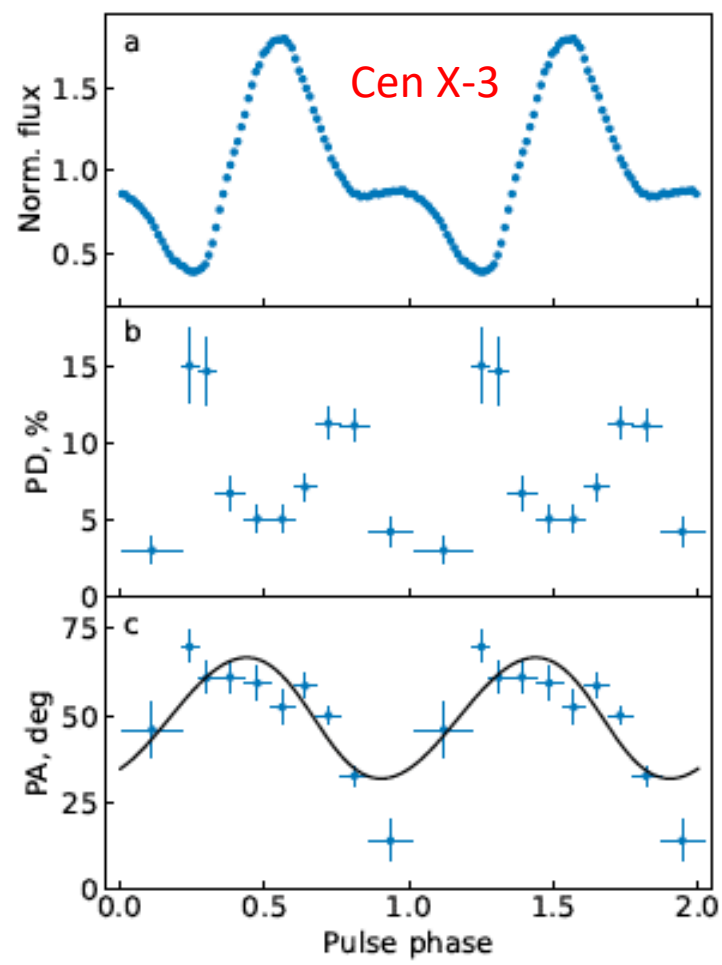
- Magnetic dipole misaligned from the rotation axis.
- Pulse phase dependence of the polarization angle (position angle of the dipole) .
- Rotating vector model of Radhakrishnan & Cooke (1969), Meszaros et al. (1988)

$$\tan(\chi - \chi_p) = \frac{-\sin \theta_p \sin \phi}{\sin i_p \cos \theta_p - \cos i_p \sin \theta_p \cos \phi}$$



χ_p - position angle of the pulsar spin
 i_p - observer inclination relative to the pulsar spin
 θ_p - magnetic obliquity
 ϕ - pulsar phase

IXPE: X-ray pulsars



■ Well fitted by the RVM

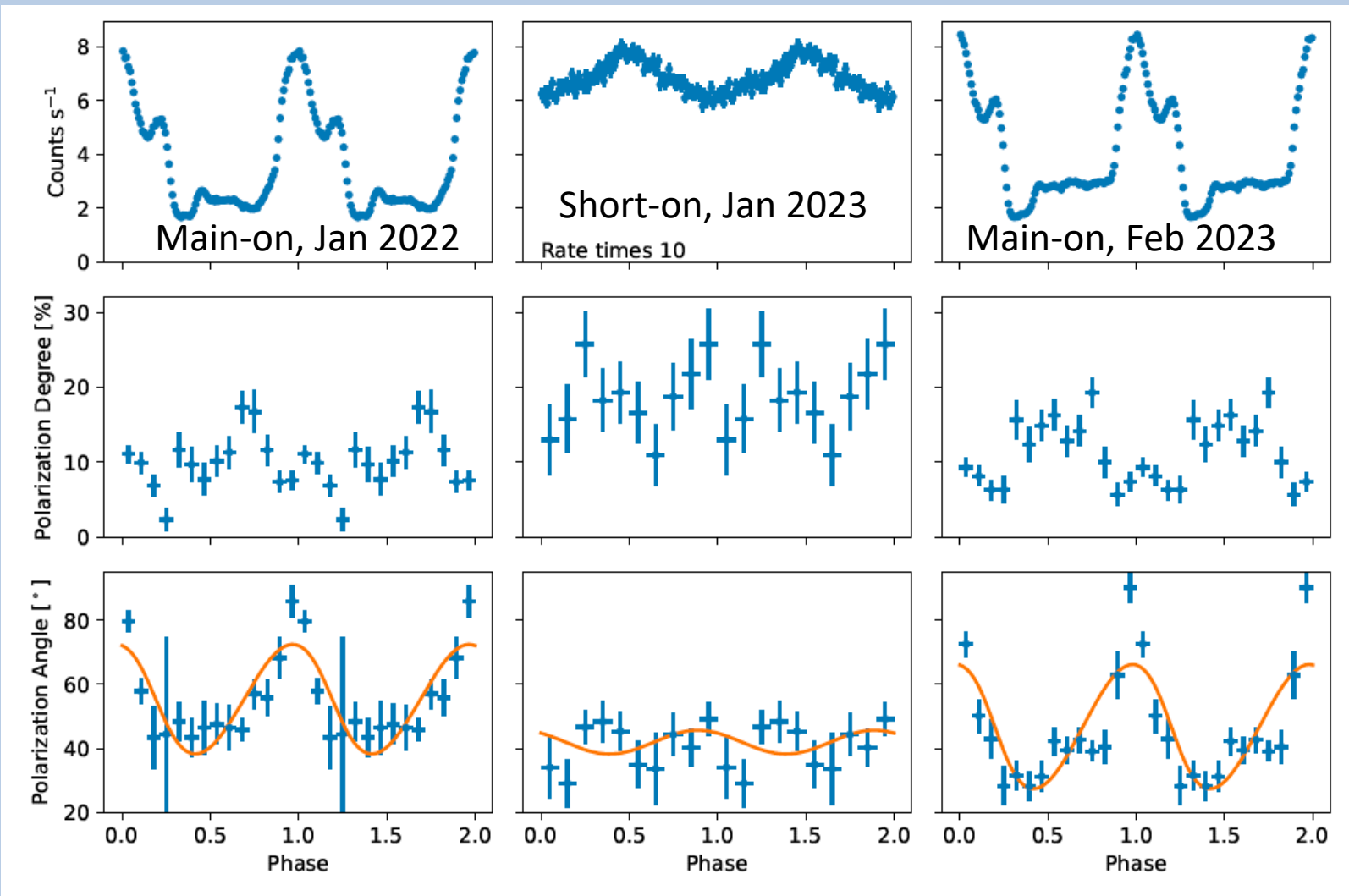
IXPE: X-ray pulsars

Table 2. RVM parameters of the XRP observed by IXPE.

Name	i_p [deg]	θ_p [deg]	χ_p [deg]
Cen X-3	70.2 (fixed)	16.4 ± 1.3	49.2 ± 1.1
Her X-1 (main-on)	56^{+24}_{-20}	$3.7^{+2.6}_{-1.9}$	42 ± 2
Her X-1 (short-on)	90 ± 30	$16.3^{+3.5}_{-4.1}$	57.9 ± 2.1
GRO J1008–57	130 ± 3	74 ± 2	75 ± 4
EXO 2030+375	128^{+8}_{-6}	60^{+5}_{-6}	-30^{+4}_{-5}
X Persei	162 ± 12	90 ± 15	70 ± 30
GX 301–2	135 ± 17	43 ± 12	135
LS V +44 17/Obs. 1	56 ± 12	27 ± 4	82 ± 1
LS V +44 17/Obs. 2	102 ± 2	54 ± 1	-6.2 ± 0.4
LS V +44 17 ^a	108 ± 2	48 ± 1	-8.4 ± 0.6
Swift J0243/Obs. 1	80 ± 3	87 ± 2	-70 ± 4
Swift J0243/Obs. 2	60 ± 5	88 ± 3	-87 ± 7
Swift J0243/Obs. 3	33 ± 7	75 ± 5	-66 ± 7
Swift J0243 ^a	25^{+8}_{-17}	77^{+2}_{-29}	-44^{+12}_{-13}
SMC X-1	91^{+41}_{-42}	13^{+7}_{-6}	87 ± 4

^a Obtained using two-component model to the combined data set.

Time dependence of X-ray polarization



Doroshenko+ 2022, Nat Astro; Heyl+ 2024, Nat Astro; Zhao+ 2024, MNRAS

Time dependence of X-ray polarization

	Mean PD	i_p	θ	χ_p	ϕ_0	Prec. Phase
	(%)	(deg)	(deg)	(deg)	(%)	(%)
First Main-On	9.5 ± 0.5	58^{+28}_{-22}	$14.5^{+3.0}_{-4.0}$	55.4 ± 1.6	$19.0^{+2.7}_{-2.2}$	8.8
Early	8.6 ± 0.6	64^{+25}_{-22}	$16.3^{+3.5}_{-4.1}$	57.9 ± 2.1	$19.0^{+2.6}_{-2.4}$	7.3
Late	9.3 ± 0.7	85^{+35}_{-37}	$15.9^{+3.6}_{-4.0}$	52.2 ± 2.7	$21.7^{+4.5}_{-5.0}$	16.2
Short-On	17.8 ± 1.4	90^{+30}_{-30}	$3.7^{+2.6}_{-1.9}$	41.9 ± 2.2	85.1^{+18}_{-19}	68.7
Second Main-On	9.1 ± 0.5	56^{+24}_{-20}	$16.0^{+3.1}_{-4.3}$	46.8 ± 1.5	$19.8^{+2.3}_{-2.0}$	15.9

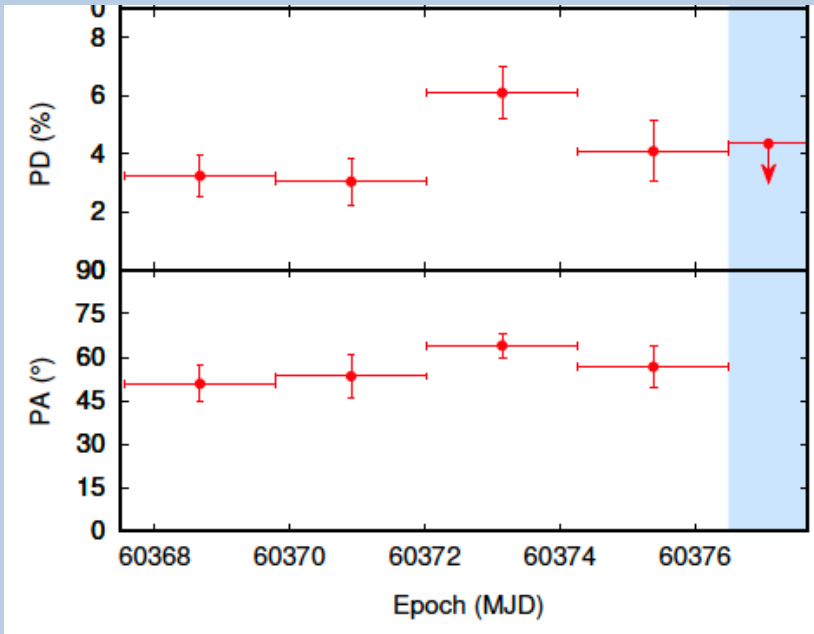
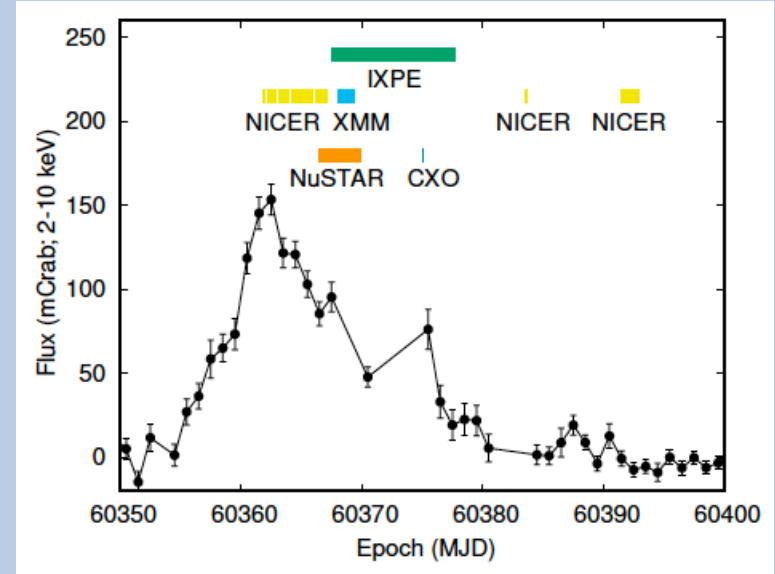
Heyl et al. 2024

Strong indication of precession!

Requires deviations from sphericity at 10^{-7} level

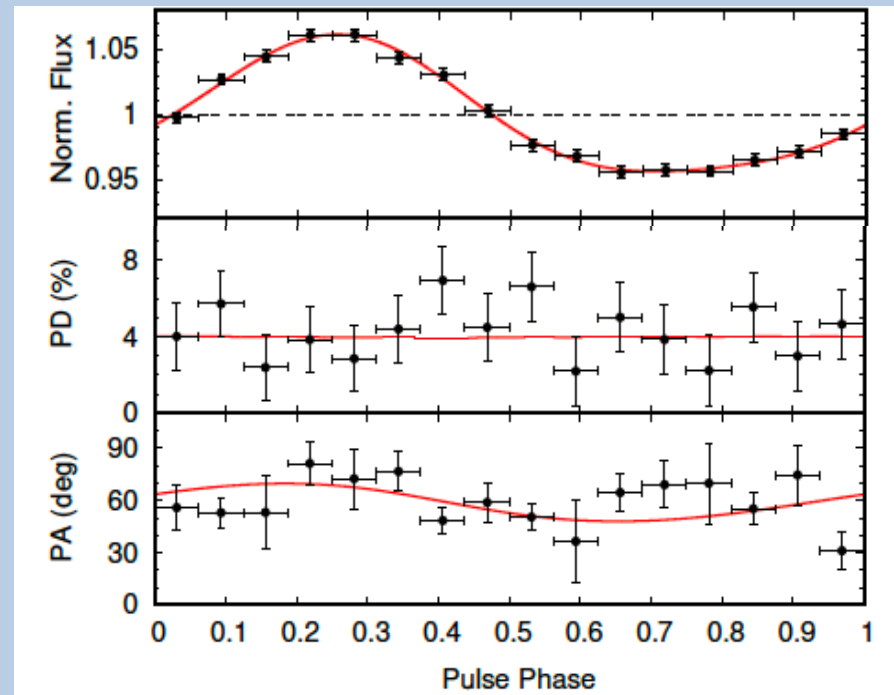
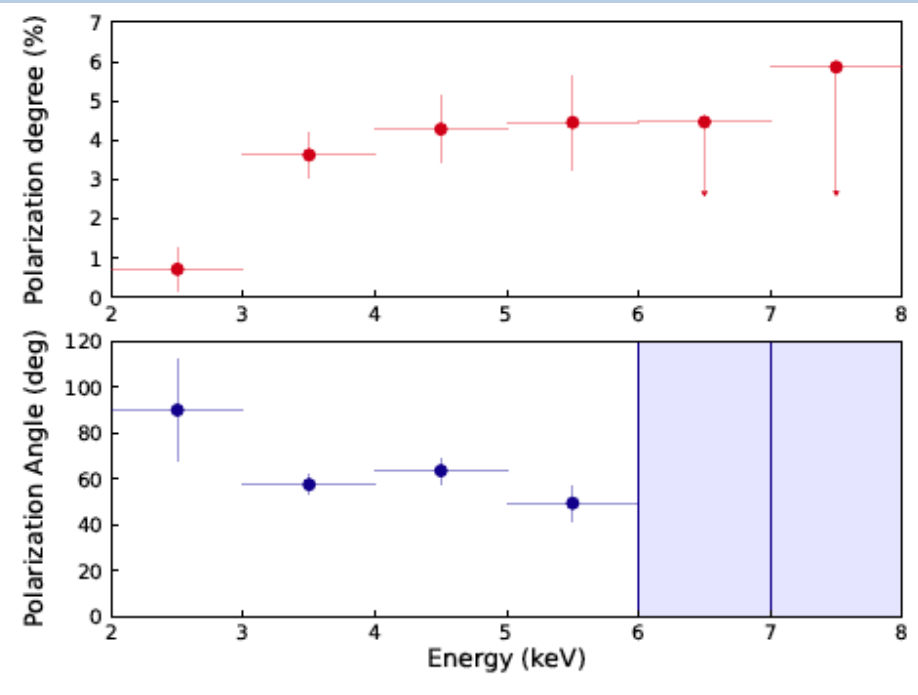
Accreting ms pulsar: SRGA J144459.2–604207

- Discovered in February 2024 by SRG/ART-XC
- Millisecond pulsations discovered with NICER
- Frequency 448 Hz
- Orbit 5.22 hr



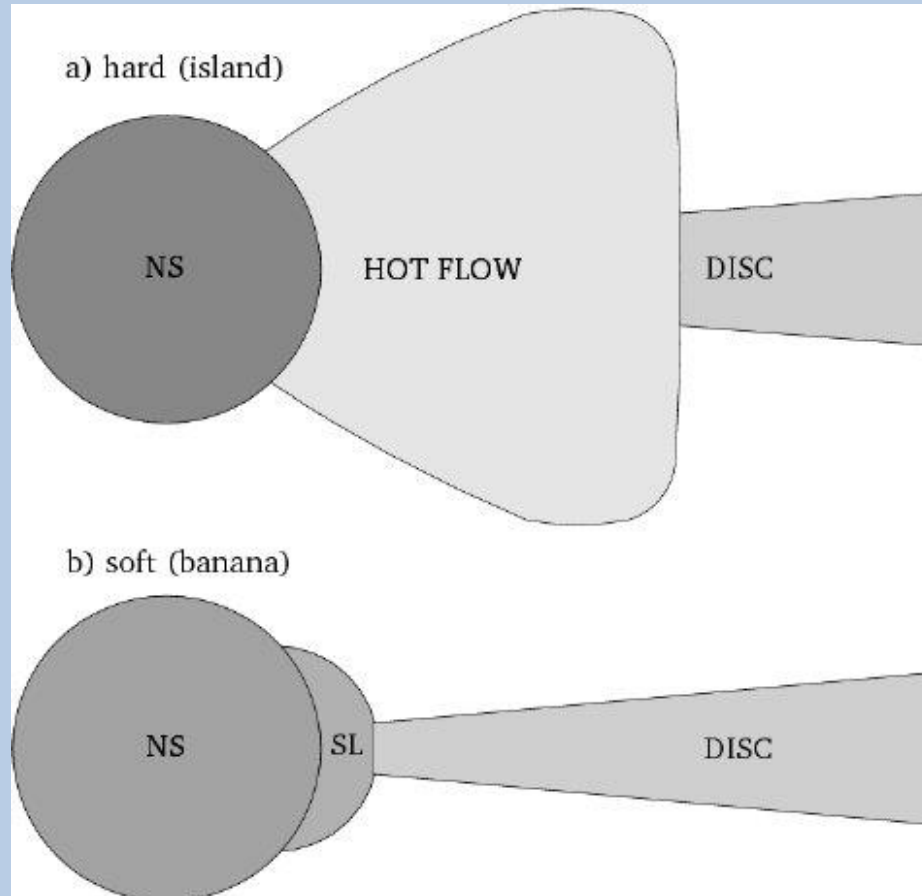
- Observed by IXPE for 10 days
- Average PD=2.3±0.4%. PA=59±6 deg

Accreting ms pulsar: SRGA J144459.2–604207

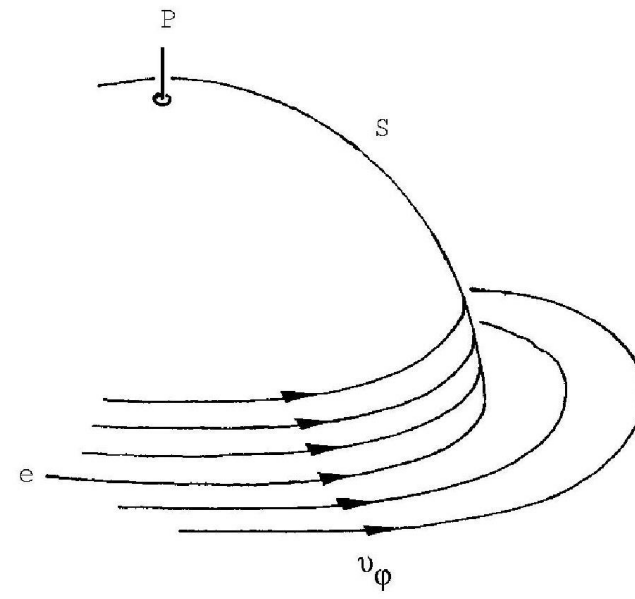
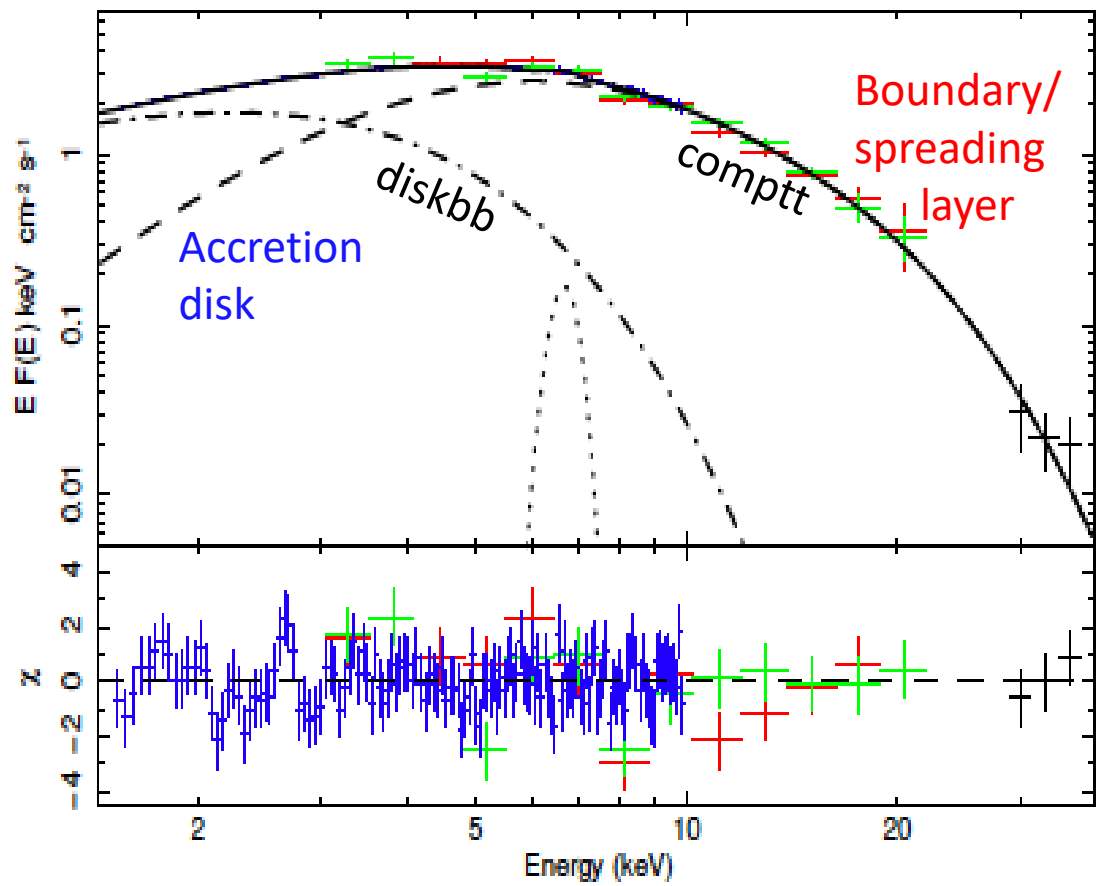


- Drop of PD below 3 keV – contribution of a thermal component
- RVM does not fit the data – more complex structure of emission region, eclipses by the accretion disk?

Non-magnetic accreting neutron stars



Nonmagnetic NS



Inogamov & Sunyaev 1999

Nonmagnetic NS: Cyg X-2

IXPE: $PD=1.8\pm 0.3\%$ at $PA=140\pm 4$ deg

OSO-8 (1976-1980):

$PD=5.0\pm 1.8\%$ at $PA=138\pm 10$ deg

Radio jet: $PA=141$ deg

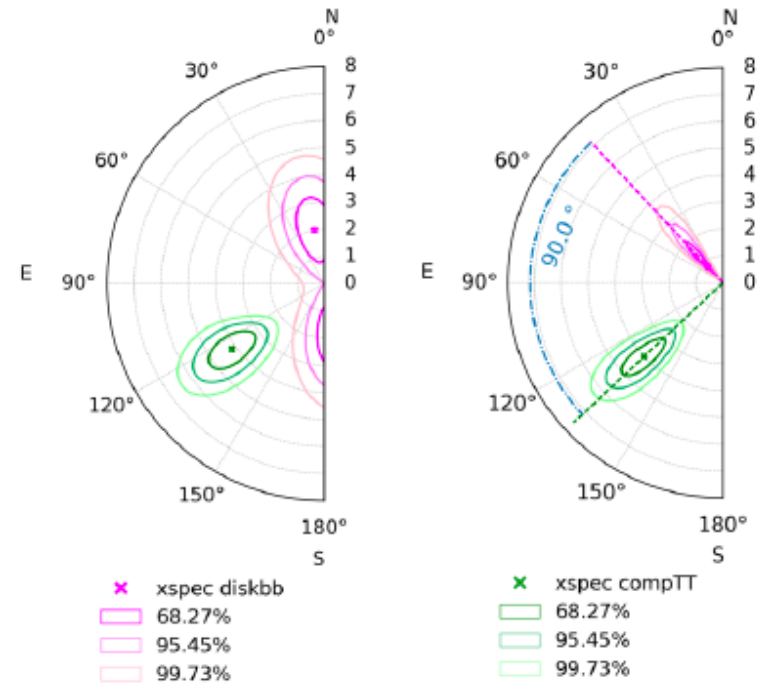
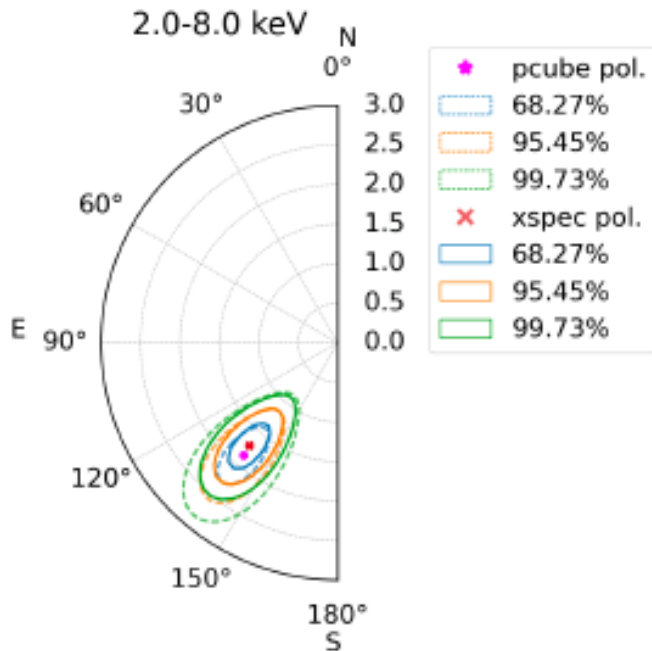
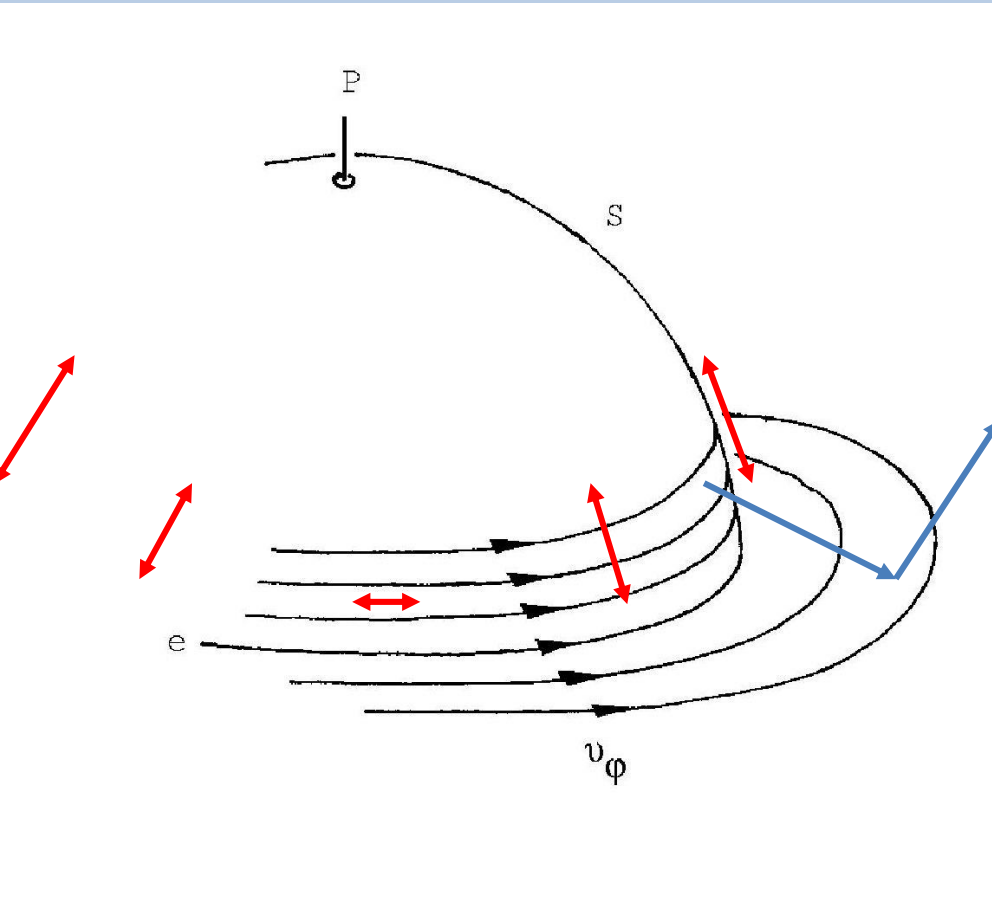


Figure 6. Contour plot of PD and PA in the 2–8 keV energy band obtained with *xSPEC*. The data have been fitted with two *polconst* models separately for the *diskbb* (pink colours) and *comptt* (green colours) components. *Left panel:* The PA of *diskbb* and *comptt* are left free. *Right panel:* The PA of *diskbb* was assumed to differ from the PA of *comptt* by 90° . Contour plots correspond to the 68.27%, 95.45% and 99.73% confidence levels, respectively.

Nonmagnetic NS: Cyg X-2



Where polarization is produced?

1. Spreading layer (Inogamov & Sunyaev 1999) ?
2. Reflection from the disk.
3. Scattering in a wind.

Polarization from the half-sphere is small. The maximum is 0.18% at $i=60$ deg (Lapidus & Sunyaev 1985).

Our new calculations show that it is difficult to get more than 1.5% even from a narrow belt.

Nonmagnetic NS: Cyg X-2

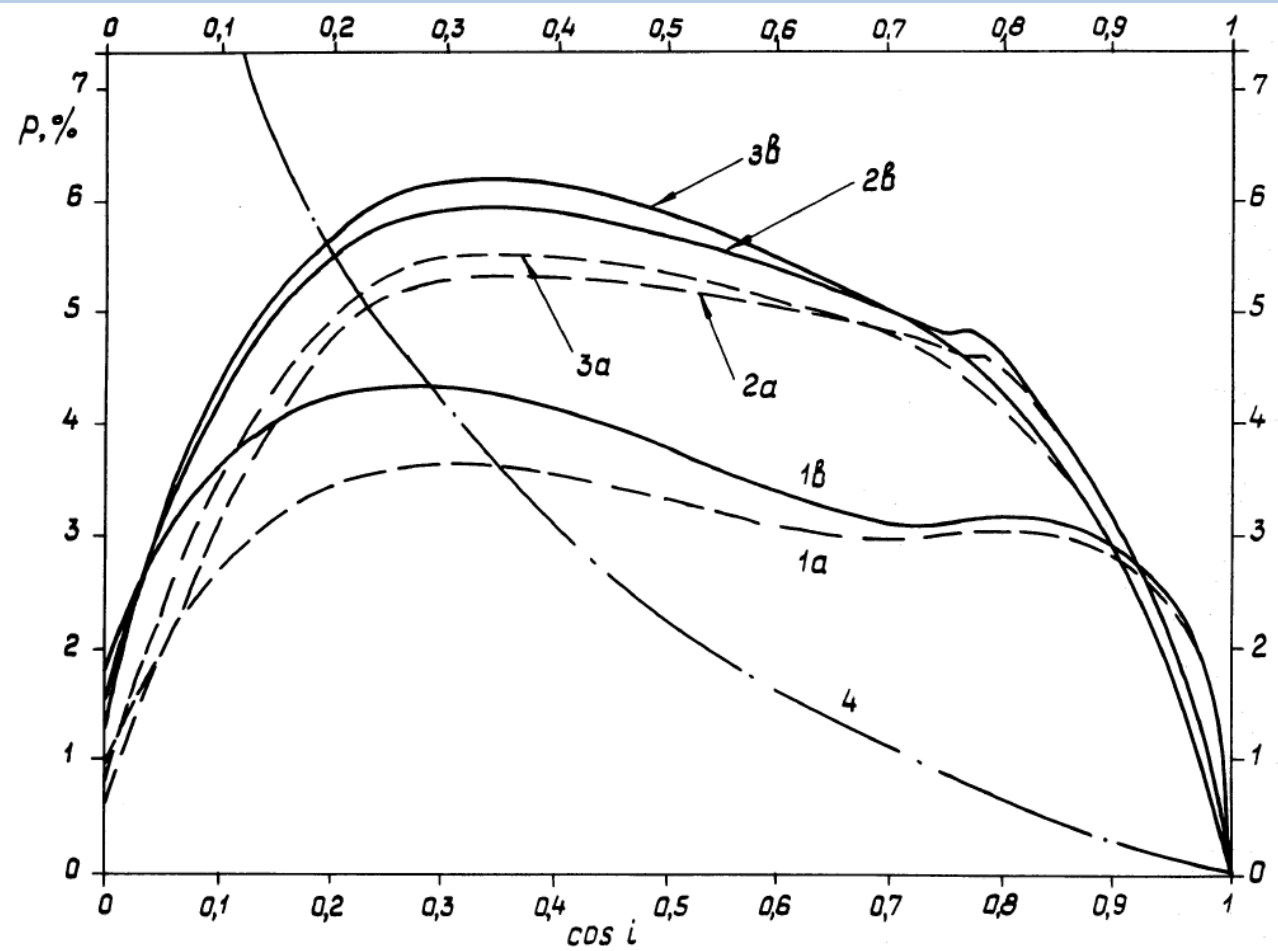


Figure 7. Degree of polarization of burster radiation between bursts. (1) $H/R_s=0.05$, (2) $H/R_s=0.1$, (3) $H/R_s=0.2$. Separately shown are (a) the polarization of disc radiation and (b) the polarization of radiation of the whole system 'disc+boundary layer'. The degree of polarization of radiation emitted by a semi-infinite electron scattering atmosphere (Chandrasekhar 1960) is also shown (4) for comparison.

2. Reflection from the accretion disk (Lapidus & Sunyaev 1985) ?

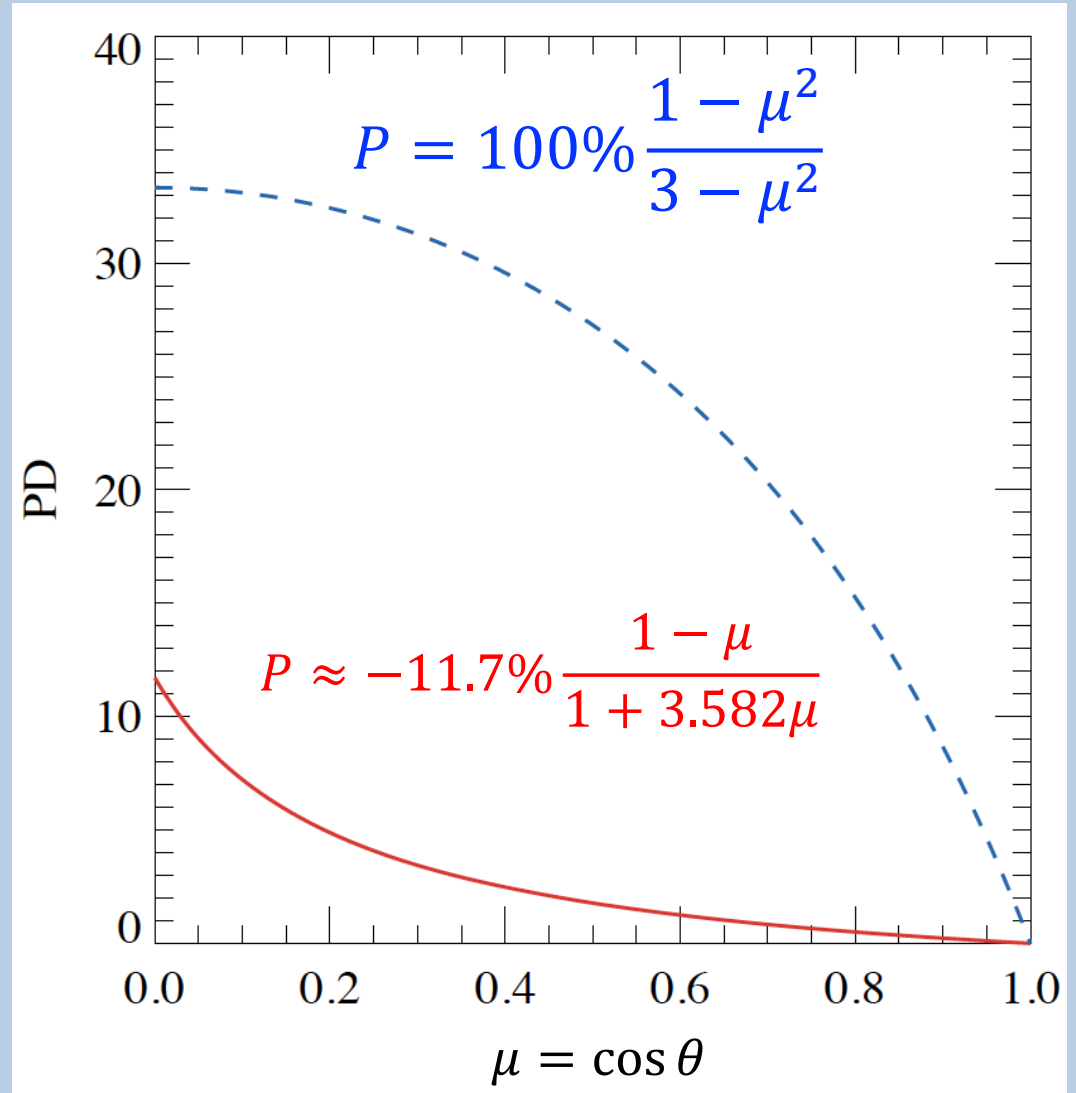
Up to 6% PD can be produced.

Models need to be updated to include relativistic effects.

Nonmagnetic NS: Cyg X-2

3. Thomson scattering in an equatorial wind (Sunyaev & Titarchuk 1985).

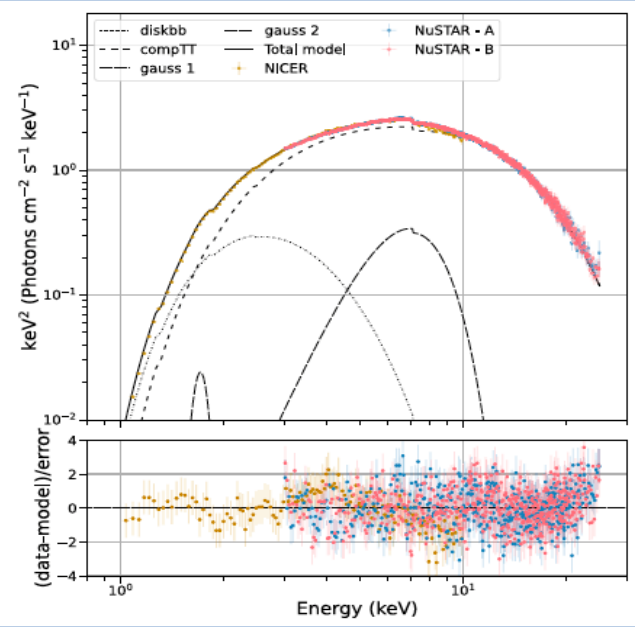
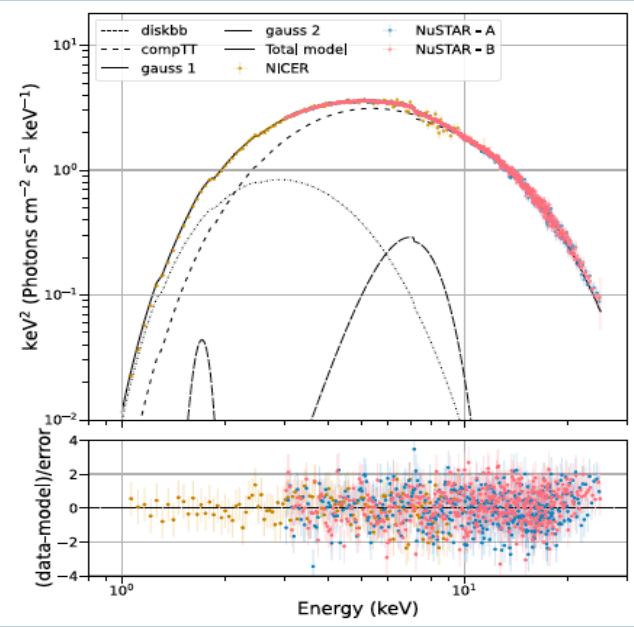
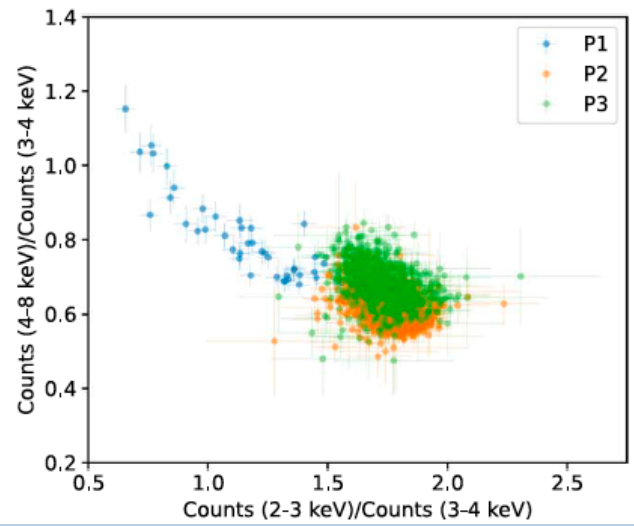
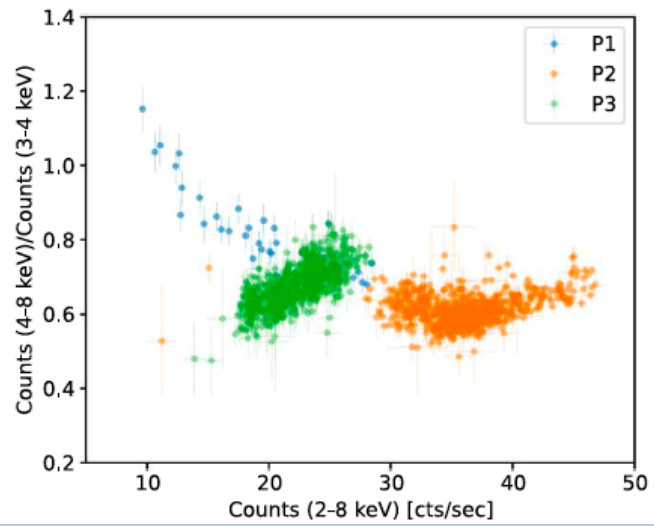
Chandrasekhar-Sobolev (optically thick electro-scattering dominated) case



Nonmagnetic NS: Cir X-1

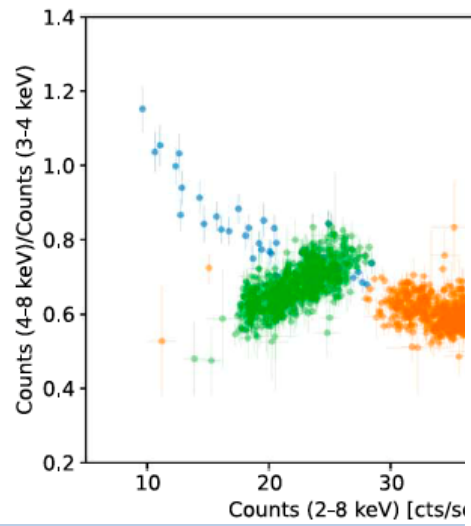
The youngest X-ray binary in the Galaxy,
<5000 yr.

Orbital period of 16.6 d.

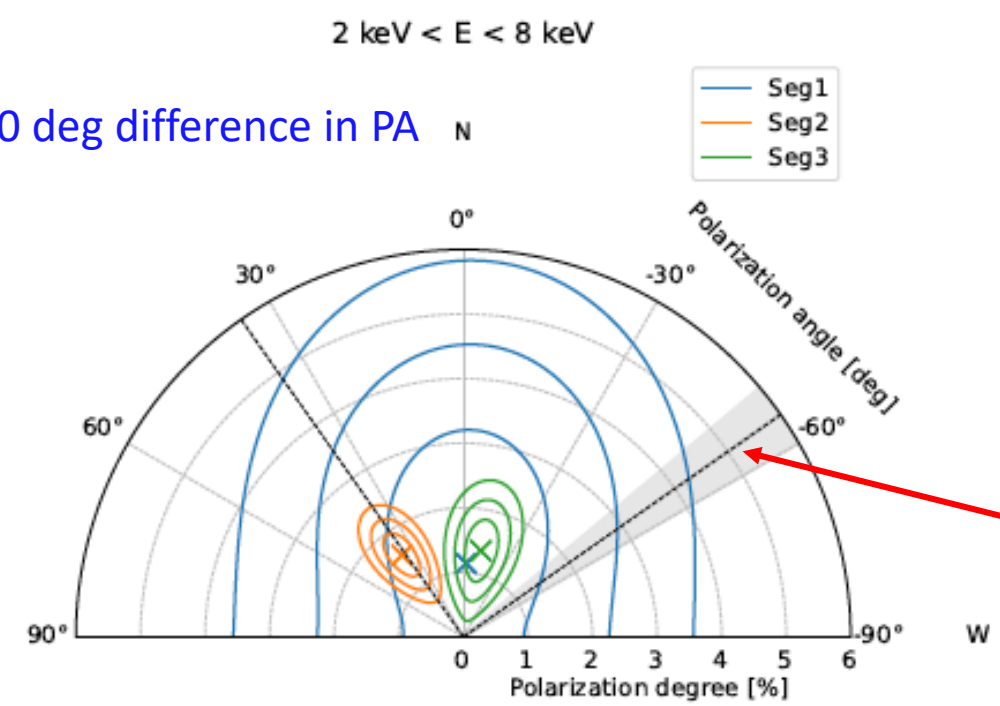


IXPE observed twice for
about 130 ks each time.

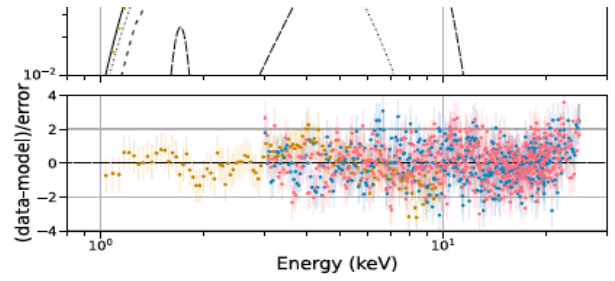
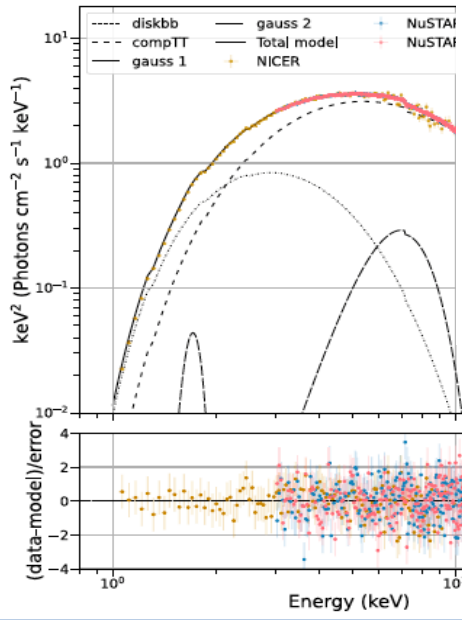
Nonmagnetic NS: Cir X-1



50 deg difference in PA

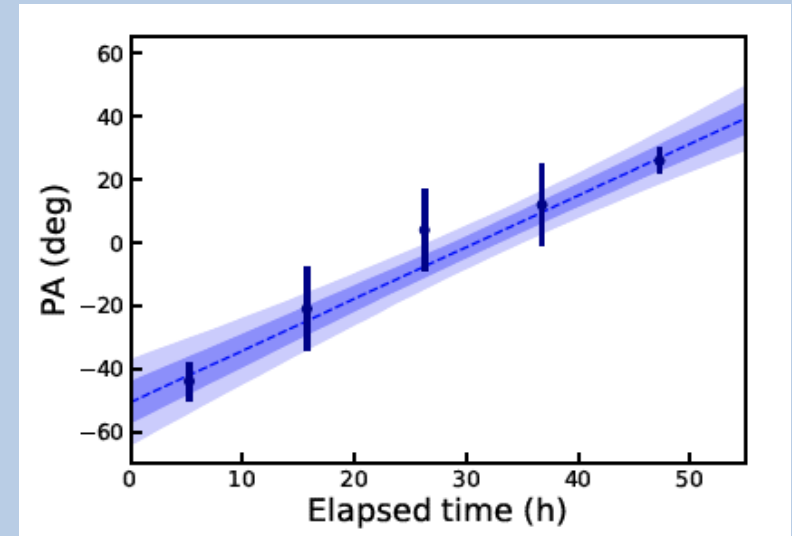
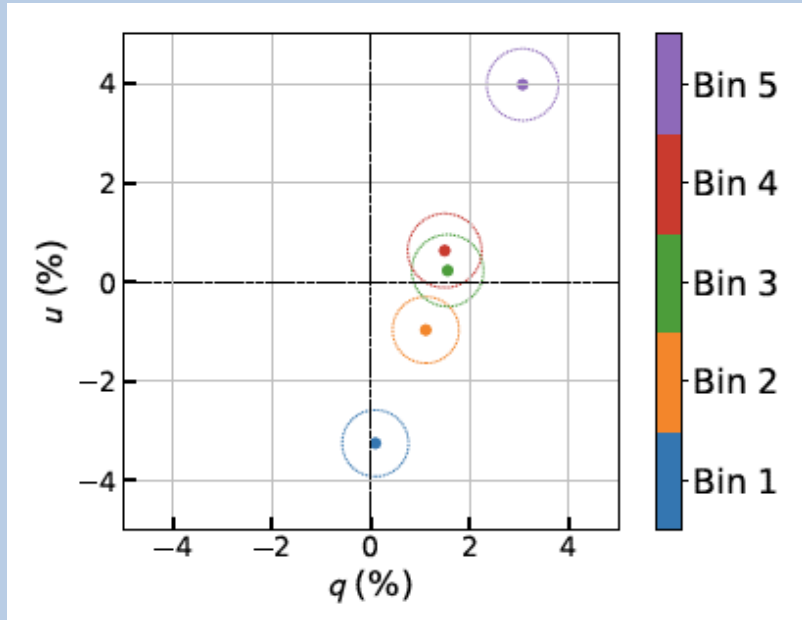
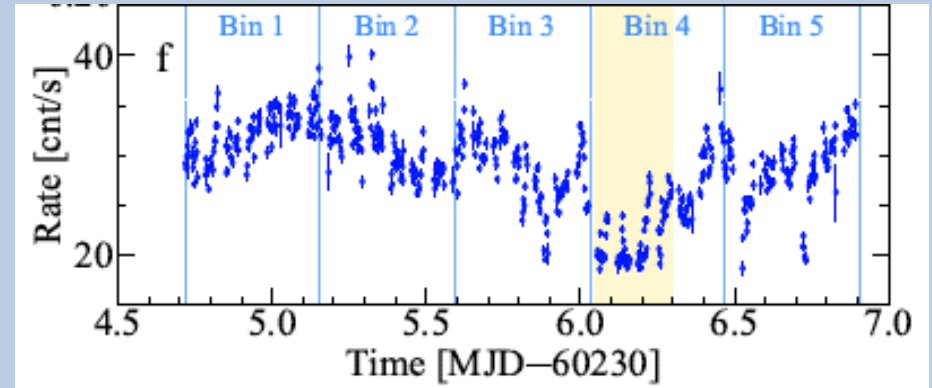


jet



Nonmagnetic NS: GX 13+1

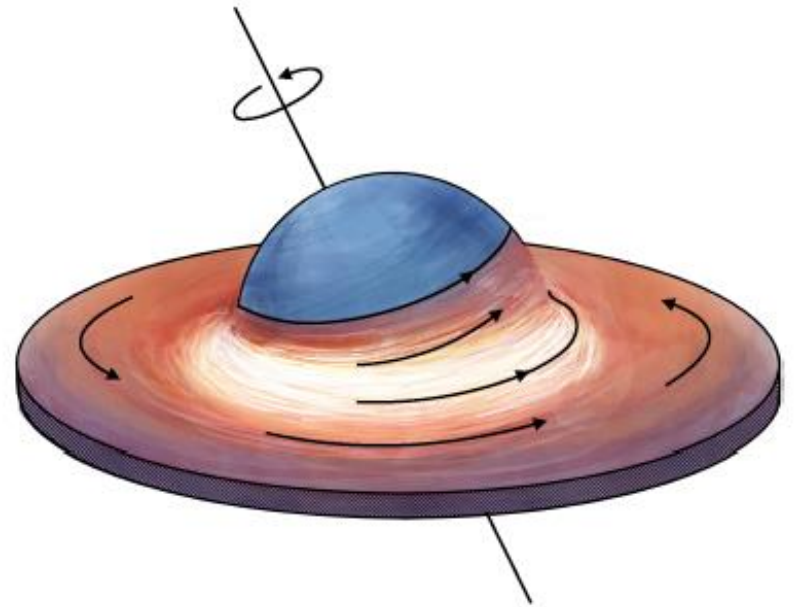
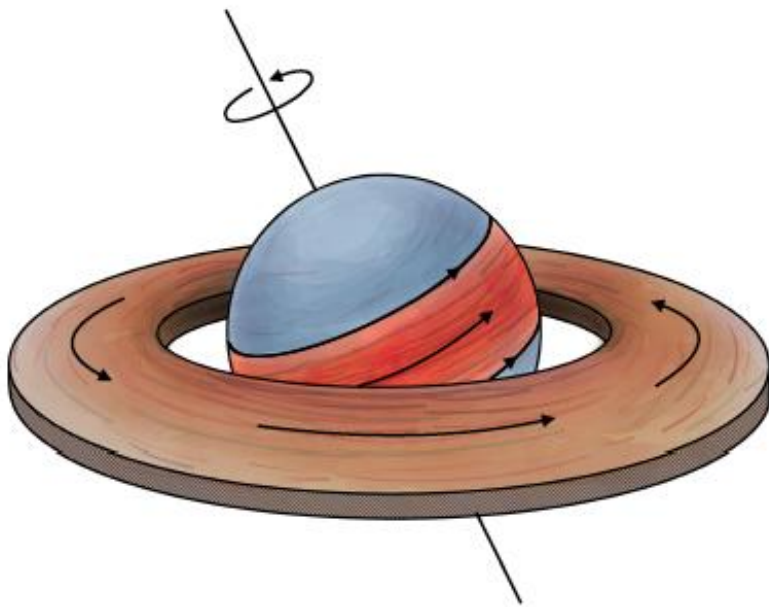
- X-ray binary, dipper
- Inclination around 70 deg
- 24.5 day orbit
- Companion K5 III
- Observed by IXPE in October 2023



Rotation of the PA by 70 deg !

Evidence for misalignment of the NS and orbital spin?

Nonmagnetic NS: geometry



Evidence for misalignment of the neutron star spin from the orbital spin.

Conclusion

- IXPE has opened a new window to the Universe.
- Observations of X-ray polarization has revolutionized our understanding of X-ray binaries.
- IXPE allows to measure geometry of emission region in accreting black holes and neutron stars.
 - In accreting black holes, emission (hot flow) region \perp jet. Lamp-post, jet - rejected. Cyg X-3 was identified as an ULX.
 - X-ray pulsar geometry was uncovered. Precession of Her X-1 confirmed.
 - Found evidence of misalignment of nonmagnetic NS.